### 2.6. Flow cytometry

Cells were labeled with PE-Cy5-conjugated anti-CD4 antibody or PE-conjugated anti-CXCR4 antibody (Beckton Dickinson, San Jose, Calif.) for 30 min at 4 °C. Cells were washed once with PBS supplemented with 1% FBS and analyzed by FACS Aria (Beckton Dickinson). The GFP-positive cells were sorted using FACS Aria.

### 2.7. Monitoring HIV-1 replication

For HIV-1 infection, $1 \times 10^5$ cells were incubated at the room temperature with the HIV-$1_{HXB2}$-containing culture supernatant, which had approximately 1.0 ng of $p24^{CA}$, for approximately 30 min. The culture supernatants were collected at 4 d post-infection and subjected to ELISA to measure the $p24^{CA}$ antigen, using a Retro TEK p24 Antigen ELISA Kit according to the manufacturer's protocol (Zepto Metrix, Buffalo, NY). The signals were measured with an ELx808 microplate photometer (BIO-TEK®, Winooski, VT).

### 2.8. PCR analysis

The cellular DNA and RNA were extracted from cells infected with VSV-G-pseudotyped HIV-1 vector produced by using pNL-Luc plasmid, as described previously [17]. The Alu-LTR PCR and RT-PCR were performed as described previously [3,17] using the following primers: for the first Alu-LTR PCR reaction, 5'-AACTAGGGAACCCACTGCTTAAG-3' and 5'-TGCTGGGATTACAGGC-GTGAG-3'; and for the second Alu-LTR PCR reaction, 5'-AACT-AGGGAACCCACTGCTTAAG-3' and 5'-CTGCTAGAGATTTTCCACA-CTGAC-3'. For amplification of HIV-1 mRNA, 5′-ATGGAGCCAGTAG-ATCCTAGAC-3′ and 5′-CTATTCCTTCGGGCCTGTCGGG-3′ primers were used. For the control, we amplified beta-globin and cyclophilin A using the following primers: beta-globin, 5'-TATTGGTCT-CCTTAAACCTGTCTTG-3' and 5'-CTGACACAACTGTGTTCACTAGC-3'; and cyclophilin A, 5′- CACCGCCACCATGGTCAACCCCACCGTGTTCT-TCGAC-3′ and 5′- CCCGGGCCTCGAGCTTTCGAGTTGTCCACAGTCA-GCAATGG-3′. The amplicons were separated in a 2% agarose gel, stained with ethidium bromide, and imaged with a Typhoon scanner (GE Healthcare Bio-Sciences).

### 2.9. Collection of virus-like particle

Tissue culture supernatants containing virus-like particles (VLP) were passed through nitrocellulose filters (0.45 μm, Millipore, Tokyo, Japan) and the virions were collected by centrifugation (Optima™ TL, TLA 100.3 rotor, 541 k × *g* for 1 h; Beckman Coulter, Miami, FL).

## 3. Results

### 3.1. Identification of SEC14L1a as a potential regulator of HIV-1 replication

We prepared MT-4 cells that constitutively express cDNA transduced by a lentiviral vector or an MLV-based retroviral vector (Fig. 1A). The cDNAs were derived from human peripheral blood mononuclear cells (PBL) and *Oryctolagus cuniculus* (European rabbit) kidney-derived cell line RK13 cells. MT-4 cells transduced with cDNA were collected by FACS sorter using the green fluorescence as a marker since viral vectors encoded the GFP expression cassette. Then, cells were infected with HIV-1. Surviving cells were propagated and the genomic DNA was extracted to recover the transduced cDNA by PCR as previously described [3]. We isolated two clones encoding the carboxy terminal domain (CTD) of SEC14L1a (Gene ID 6397, Fig. 1B and C); one from the PBL cDNA library (1/65 independent clones, 1.5%), and one from the RK13 cDNA library (1/42 independent clones, 2.4%). The fact that the SEC14L1a CTD was successfully identified from two independent cDNA libraries strongly suggests that it is a negative regulator of HIV-1 replication. It is important to note that previous genome-wide screenings for HIV-1 regulators have not identified SEC14L1a CTD. This clearly suggests that our T cell-based cDNA screening system is unique, and should be able to complement the other genome-wide screening systems.

SEC14L1a belongs to the widely-expressed SEC14-superfamily that is involved in membrane trafficking and phospholipid metabolism [18–21]. The function of SEC14L1a is not well understood. The C-terminus of SEC14L1a encodes a Golgi dynamics (GOLD) domain (amino acids (aa) 523–674; Fig. 1C) that mediates the protein-protein interaction possibly involved in the maintenance of Golgi apparatus function and vesicular trafficking [22]. The only reported biological activity of SEC14L1a is to interact with cholinergic receptors AchT and CHT1 [23]. The GOLD domain is responsible for the physical interaction between SEC14L1a and cholinergic receptors. However, the functional significance of these interactions remains to be clarified. The conserved SEC14 domain directly interacts with lipid molecules [17–21]. However, the lipid ligand of SEC14L1a (aa 319–490, Fig. 1C) has yet to be identified.

### 3.2. Construction of expression vectors for SEC14L1a derivatives

The longest SEC14L1a cDNA recovered from the PBL cDNA library spanned nucleotides (nt) 2045–2492 of SEC14L1a mRNA (NM_003003.3), covering the CTD of the SEC14L1a open reading frame (ORF; Fig. 1B). We detected a potential translational start codon at nt 2188-2190 within the GOLD domain (asterisk, Fig. 1B). We speculated that the isolated cDNA might have expressed the carboxy half of the GOLD domain (aa 641–715) in MT-4 cells, leading to the inhibition of HIV-1 replication.

To test this, we constructed an expression plasmid for FLAG-tagged CTD (aa 642-715) fused to the carboxy terminus of GFP (CTD1; Fig. 1C). We also constructed GFP fusion proteins spanning the GOLD domain (CTD2, aa 493–715) or the full-length SEC14L1a (FL; Fig. 1C). Expression of these proteins was verified by Western blotting of transient transfected 293T cells (Fig. 1D). The confocal microscopy analysis indicated that the FL localized mainly in the cytoplasm, with some accumulation in the perinuclear regions (Fig. 1E), consistent with a previous report [23]. CTD1 was distributed in the cytoplasm and the nucleus, with a slight preference for the cytoplasm. CTD2 was evenly distributed to the nucleus and cytoplasm. When MT-4 cells constitutively expressing FL, CTD1, and CTD2 were analyzed, the subcellular distribution was less clear, due to the small cytoplasm (Fig. 1F). However, FL was distributed evenly to the nucleus and cytoplasm in MT-4 cells. In contrast, CTD1 was excluded from the nucleus in MT-4 cells (Fig. 1F). The distribution of CTD2 in MT-4 cells was similar to that in 293T cells (Fig. 1F). The differences of protein distribution in two cell types may be caused by the cell type-dependent regulation of protein trafficking and/or the effect of protein expression levels.

### 3.3. Verification of anti-HIV-1 activity associated with SEC14L1a CTD1

We introduced FL, CTD1, or CTD2 into MT-4 cells using the MLV vector, and isolated cells constitutively expressing FL, CTD1, or CTD2. Expression of SEC14L1a derivatives in MT-4 cells was verified by Western blotting (Fig. 2A). FL expression was verified by immuno-precipitation assay (Fig. 2A). The detection of FL by Western blotting was inefficient considering the fact that all the SEC14L1a derivatives are GFP-tagged, and the GFP intensity of FL-expressing MT-4 cells was not lower than that of CTD1-expressing

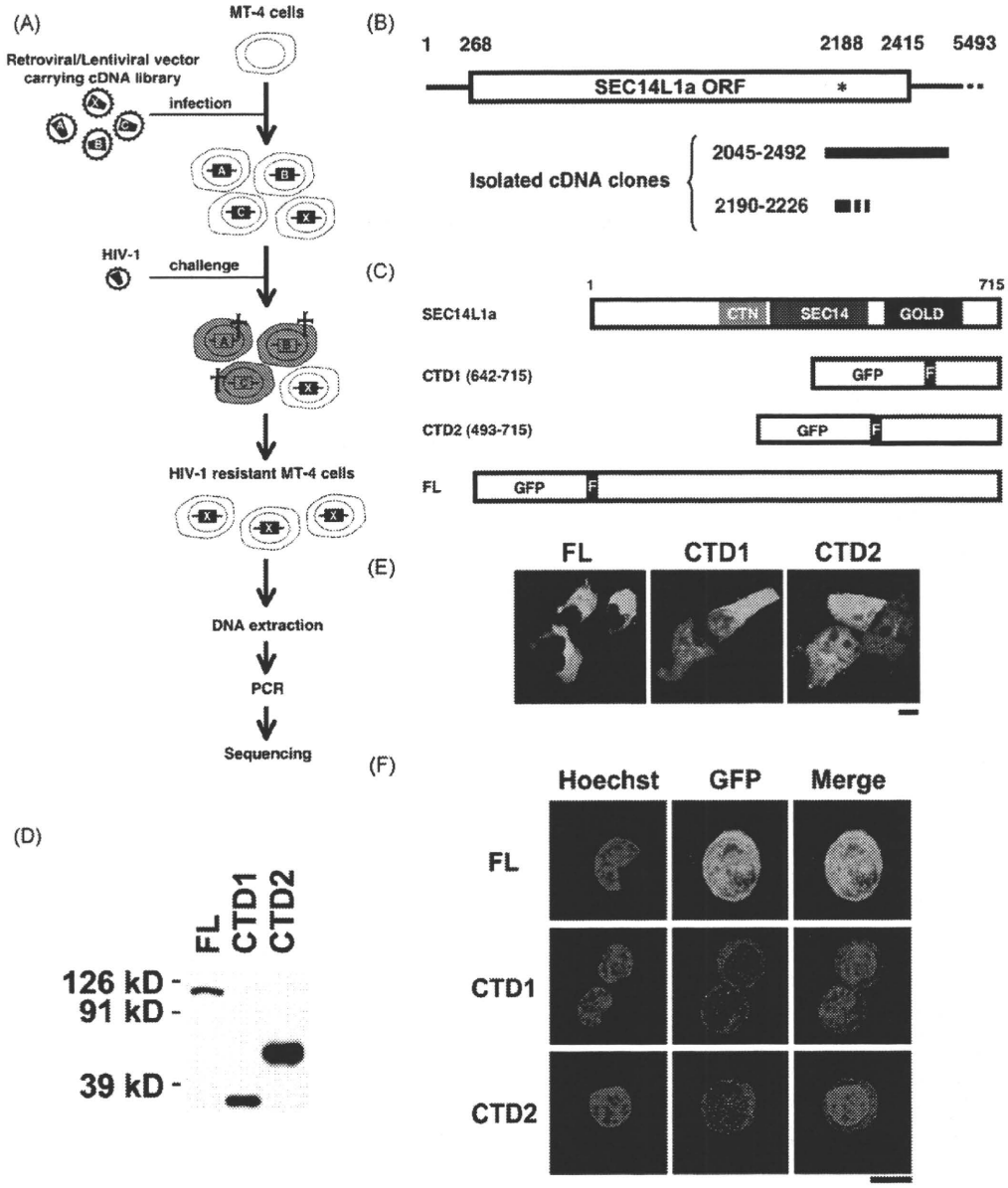


**Fig. 1.** Identification of SEC14L1a CTD as a potential regulator of HIV-1 replication. (A) The experimental strategy used to screen a cDNA library for genes rendering cells resistant to HIV-1. MT-4 cells were infected with a retroviral or lentiviral vector carrying cDNA libraries and were challenged with wild-type HIV-$1_{HXB2}$. The HIV-1-infected cells (gray with cross) quickly undergo cell death. The surviving cells were propagated, collected, and the transduced cDNA labeled X was determined. (B) Schematic representation of SEC14L1a mRNA (NM_00303.3) and the isolated gene fragments. The open reading frame (ORF) is assigned from nucleotides (nt) 268 to 2415. The potential internal translational initiation codon is marked with an asterisk. (C) Schematic representation of the SEC14L1a protein (NP_002994). SEC14L1a has a CRAL_TRIO_N domain (CTN, amino acids 241–313), a SEC14p-like lipid-binding domain (SEC14, amino acids 319–490), and a Golgi dynamics domain (GOLD, amino acids 523–674). The cloned fragments (CTD1 and CTD2) and full-length (FL) gene were tagged with a FLAG epitope (indicated with an "F") on their N-termini, and fused to the C-terminus of GFP. (D) Verification of FL, CTD1, and CTD2 expression in 293T cells by Western blotting using anti-FLAG antibody. (E) Confocal microscopy images of 293T cells expressing FL, CTD1, or CTD2. The green signal represents GFP fluorescence. Magnification, 630×; scale bar, 10 μm. (F) Confocal microscopy images of MT-4 cells constitutively expressing FL, CTD1, or CTD2. The blue signal represents the Hoechst-stained nucleus, and green represents GFP fluorescence. Magnification, 630×; scale bar, 5 μm.

cells (Fig. 1F). The MLV vector expressing GFP alone was used as a control. The cell proliferation, morphology, and cell surface levels of HIV-1 receptors were unaltered by any of the SEC14L1a derivatives (Fig. 1F, 2B, and data not shown). HIV-1 replication was tested in these cells. The level of HIV-1 replication was significantly inhibited in CTD1- and CTD2-expressing cells (69.1% and 69.8% on the average from seven independent experiments, respectively, $P < 0.05$, two-tailed Student's $t$-test), but was hardly inhibited in FL-expressing cells (86.4%, not statistically significant; Fig. 2C). This observation was reproducible in independently established MT-4 cells and SupT1 cells (data not shown). These data verified the original screening results, and suggest that the C-terminal half of GOLD domain of SEC14L1a serves as an inhibitor of HIV-1 replication. In contrast, it is suggested that FL is not a potent negative regulator of HIV-1 replication.

### 3.4. SEC14L1a CTD1 and CTD2 target the late phase of the HIV-1 life cycle

We analyzed the viral entry and production phases to determine which step of the HIV-1 life cycle CTD1 and CTD2 target.

The Alu-LTR PCR assay was performed to examine the effect of SEC14L1a derivatives on the viral entry phase. The MT-4 cells stably expressing GFP, FL, CTD1, or CTD2 were infected with VSV-

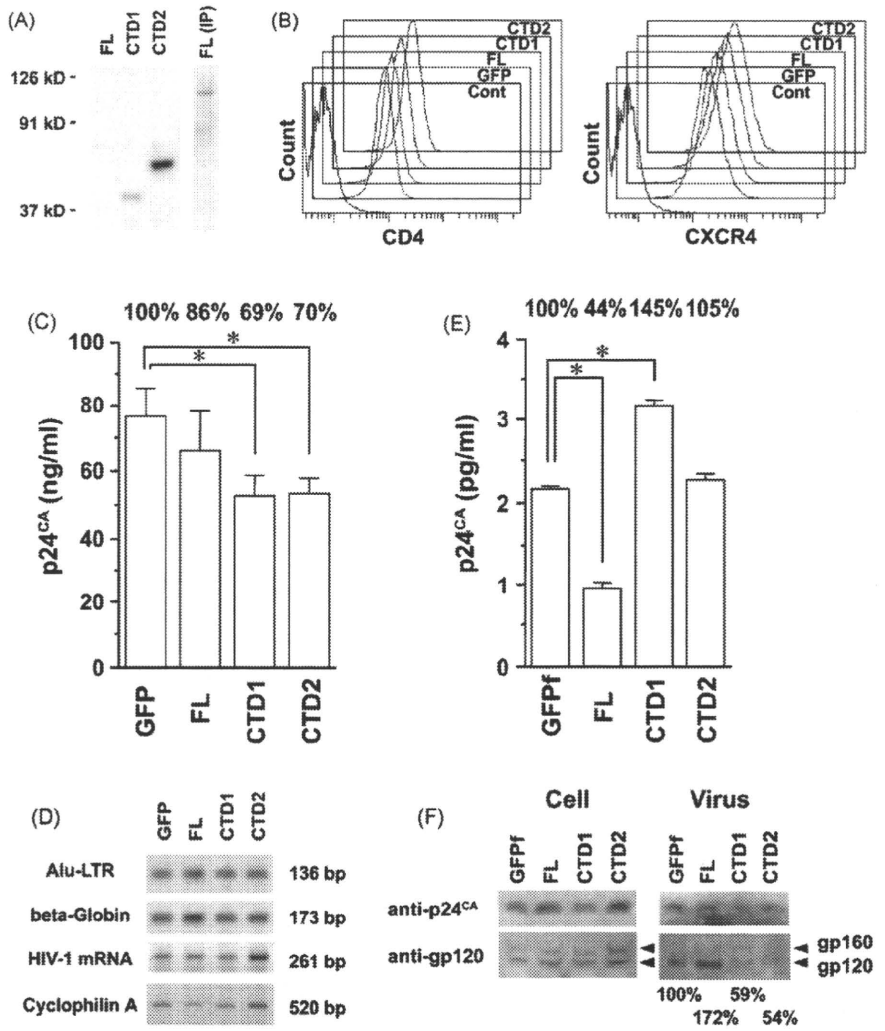


**Fig. 2.** Functional characterization of the SEC14L1a derivatives. (A) Detection of stable expression of FL, CTD1, and CTD2 in MT-4 cells by Western blotting using anti-FLAG antibody. FL was detected by the immunoprecipitation (IP) assay using agarose beads conjugated with anti-FLAG antibody. The flow cytometric analysis of the cell surface expression of HIV-1 receptors CD4 and CXCR4 in MT-4 cells stably expressing GFP, FL, CTD1, and CTD2. (C) Constitutive expression of CTD1 and CTD2 limited the replication of HIV-1 in MT-4 cells. The concentration of viral $p24^{CA}$ antigen in the culture supernatant was measured at 4 d post-infection. The results represent the average of seven independent experiments ± the standard error of the mean. The reduction of viral $p24^{CA}$ concentration relative to GFP was shown on the top. Asterisks indicate the statistical significance compared to GFP ($P < 0.05$ by two-tailed Student's *t*-test). (D) The PCR-based assay to examine the effect of SEC14L1a derivatives on the early phase of viral life cycle (top two panels) and the transcription from LTR promoter (bottom two panels). The HIV-1 entry efficiency was examined by Alu-LTR PCR. Beta globin was used as an internal control. The HIV-1 transcription efficiency was examined by RT-PCR targeting spliced viral mRNA. Cyclophilin A was used as a control. The expected length of each PCR amplicon was indicated. (E) The effect of SEC14L1a derivatives on the HIV-1 production. The 293T cells grown in a well of a 6-well plate were transfected with 200 ng of HIV-1 proviral DNA and 2 μg of expression vector for GFPf, FL, CTD1, or CTD2. The culture supernatant was recovered at 2 d post-transfection and the $p24^{CA}$ concentration was measured. The representative data from five independent experiments was shown. The results indicate the average ± the standard deviation. The relative $p24^{CA}$ concentration compared to GFPf was shown on the top. Asterisks indicate the statistical significance compared to GFPf ($P < 0.001$ by two-tailed Student's *t*-test). The *Env* incorporation onto the virus-like particles (VLP) produced by 293T cells expressing SEC14L1a derivatives. The 293T cells grown in a well of a 6-well plate were transfected with 1 μg of *gag-pol* (pCMVR8.91) and *Env* (pIIIex) expression vectors along with 2 μg of expression vector for GFPf, FL, CTD1, or CTD2. The cell lysates (Cell) and VLP fractions (Virus) were subjected to Western blot analysis detecting gp120 and $p24^{CA}$ harvested at 2 d post-transfection. The *Env* incorporation levels normalized to $p24^{CA}$ relative to GFPf were shown at the bottom.

G-pseudotyped HIV-1 vector, and the cellular genomic DNA was recovered at 4 d post-infection. The amount of Alu-LTR PCR products from FL-, CTD1-, or CTD2-expressing MT-4 cells was almost equal to that from GFP-expressing cells, suggesting that the early phase of the viral life cycle is not inhibited by any of the SEC14L1a derivatives (Fig. 2D). To examine the viral production phase, we examined the LTR-driven viral gene transcription by RT-PCR. Cellular RNA was extracted from the same MT-4 cells infected with VSV-G-pseudotyped HIV-1 vector, and RT-PCR was conducted to amplify LTR promoter-driven spliced HIV-1 mRNA. The amount of viral RNA expressed in FL-, CTD1-, or CTD2-expressing cells was not lower than that in GFP-expressing cells when the levels of the internal control was taken into account (Fig. 2D). Given that the similar number of viral genome was integrated as indicated by the Alu-LTR PCR, these data suggest that viral transcription is not inhibited by any of the SEC14L1a derivatives, and that the action point of CTD1 and CTD2 should be at post-transcriptional levels of the viral production phase.

Next, the FL, CTD1, or CTD2 expression vector was co-transfected with HIV-1 proviral DNA into 293T cells, and viral production was quantified by $p24^{CA}$ ELISA. The FLAG-tagged GFP (GFPf) was used as a control hereafter. We found that the FL expression significantly reduced the production of HIV-1 (44.2%, $P < 0.001$, two-tailed Student's *t*-test) compared to the GFPf control (Fig. 2E). In contrast, the CTD1 enhanced the production of HIV-1 (145.9%, $P < 0.001$, two-tailed Student's *t*-test; Fig. 2E). However, CTD2 did not measurably affect the HIV-1 production (105.1%, not statistically significant; Fig. 2E). As the ELISA assay examines the effect

of CTDs on *Gag* functions, we next tested the functional interaction between CTDs and *Env*. The *Env* incorporation onto the virion was examined by tripartite-transfection of expression vectors for *Env*, *gag-pol*, and SEC14L1a derivatives into 293T cells, and the VLP was collected by centrifugation. The immunoblotting against gp120 was performed on the cell lysate and the VLP fraction. The cellular *Env* and *Gag* expressions were not detectably affected by any of the SEC14L1a derivatives (Fig. 2F, left panel). The *Env* incorporation onto the VLP was slightly enhanced by FL (157%; Fig. 2F, right panel). In contrast, the VLP produced from CTD1- or CTD2-expressing cells incorporated substantially fewer *Env* than those from GFPf-expressing cells (59% or 54%, respectively; Fig. 2F, right panel). These data were reproducible in independently performed experiments. The densitometric analysis of Western blot image showed that the average ± the standard error of the mean of Env incorporation onto the virion was 129.7 ± 39.9%, 54.8 ± 24.7%, and 25.5 ± 10.3% for FL, CTD1, and CTD2 compared to GFPf, respectively (3–4 independent experiments). The *Env*-mediated cell-to-cell fusion assay indicated that SEC14L1a derivatives did not limit the cell surface targeting and function of *Env* (data not shown). In addition, the *Gag* processing in virion was unaffected by any of the SEC14L1a derivatives (data not shown). Collectively, these data suggest that the HIV-1 replication is inhibited by CTD1 and CTD2 due to the inefficient *Env* incorporation onto the virion. To test this possibility, we infected fresh MT-4 cells with the equal amount of HIV-1 propagated in CTD1- or CTD2-expressing MT-4 cells (1–2 ng $p24^{CA}$), and the viral replication was monitored at 3–4 days post-infection by measuring the $p24^{CA}$ concentration. The infectivity of HIV-1 propagated in CTD1- or CTD2-expressing cells was attenuated to 83.1 ± 17.9% or 82.4 ± 5.5% relative to the virus recovered from GFP-expressing cells, respectively (the average ± the standard error of the mean of 3 independent experiments). Altogether, these data suggest that the inhibition of HIV-1 replication by CTD1 and CTD2 is attributed to the attenuation of viral infectivity by lowering the *Env* incorporation onto the virion.

## 4. Discussion

In the present study, we provide the first evidence that the C-terminal fragment of SEC14L1a functions as an inhibitor of HIV-1 replication. The advantage of this system is that, since MT-4 cells are stably transduced with a cDNA library, the anti-HIV-1 function of a candidate gene is not due to a perturbed cell physiology. This system has been successful in identifying CD14, CD63, and Brd4-CTD as regulators of HIV-1 replication [1,3,4], and more candidates are being analyzed. Among the candidates, SEC14L1a CTD appeared to be one of the relatively modest inhibitors of HIV-1 replication. However, of note, the SEC14L1a derivatives have not been identified in other genetic screening systems. These facts point that our T cell-based system is sensitive in detecting the modest anti-HIV-1 activity of a gene, and is a unique tool in the pursuit of HIV-1 regulatory factors to complete the HIV-1-host interactome.

SEC14L1a may affect the Golgi-mediated vesicular trafficking since SEC14L1a lowers the cell surface levels of cholinergic transporters [23]. However, we do not have any data to suggest that SEC14L1a and its derivatives affect the cell surface targeting of membrane proteins including CD4, CXCR4 and *Env*. These data suggest that SEC14L1a's effect on cholinergic receptor expression is specific, and that the CTD's ability to inhibit HIV-1 replication is independent from SEC14L1a's regulatory functions on vesicular trafficking. The action point of CTD1 and CTD2 was shown to be the late phase of the viral life cycle. Given that CTD1 and CTD2 did not inhibit the biogenesis and the cell surface targeting of *Gag* and *Env*, the major mechanism of CTD1 and CTD2 to inhibit HIV-1 replication was to reduce the infectivity of HIV-1 by limiting the *Env* incorporation onto the virion. Consistent with this idea, the viral infectivity of virions produced in CTDs-expressing cells was attenuated. Then, how do CTDs block the *Env* incorporation onto the virion? We detected a weak interaction between *Gag* and CTD1 or CTD2 by immuno-coprecipitation analysis. Thus, we speculate that the interaction between *Env* and *Gag* at the plasma membrane is interfered by *Gag*-CTDs interaction, resulting in the reduction of *Env* incorporation onto the virion.

The CTD1 was an inhibitor of HIV-1 replication. While the CTD1 negatively affected the *Env* incorporation onto the virion, it positively affected the HIV-1 production. These observations may be seemingly controversial. However, the SEC14L1a derivatives' effect on HIV-1 replication is a summation of their effects of on each step of the viral life cycle. Therefore, it is conceivable that CTD1 can serve as a negative regulator of HIV-1 replication as well as a positive and negative factor on distinct steps of the viral life cycle. These seemingly controversial findings may be in part due to the cells in which the biological functions of SEC14L1a derivatives were examined. The effect of SEC14L1a derivatives on HIV-1 replication was investigated in MT-4 cells, whereas those on the HIV-1 production and *Env* incorporation onto the virion were examined in 293T cells. Although the basic biological features are largely shared among different cell types, it is possible that the SEC14L1a derivatives may function slightly differently in MT-4 cells from 293T cells given that the intracellular distribution of SEC14L1a derivatives in MT-4 cells was not identical to that in 293T cells (Fig. 1E and 1F).

Elucidating the molecular mechanism underlying CTDs' activity not only provides a hint to understand how the HIV-1 virion actively uptakes *Env* through the *Gag-Env* interaction, but also leads to the development of a novel anti-retroviral drug that lowers the infectivity of the virus by preventing *Env* incorporation onto the virion. This is the strength of our T cell-based assay since CTDs inhibit HIV-1 replication specifically. In the previous study, we proposed that a small portion of Brd4 may serve as a therapeutic molecular target for HIV-1 infection, since the constitutive expression of Brd4-CTD limited HIV-1 replication specifically [3], akin to the SEC14L1a CTDs. However, it remains to be examined whether the SEC14L1a and Brd4 derivatives inhibit HIV-1 replication in primary HIV-1 target cells.

The genome-wide screening has potential caveats, including a cDNA bias and a cell line bias. A cDNA library is not a perfect representation of mRNA expressed in the cells from which the library is constructed. For example, the longer the mRNA, the less efficiently the full-length cDNA is synthesized. In fact, we isolated Brd4-CTD from the PBL cDNA library as a potent inhibitor of HIV-1 replication [3]. However, although Brd4 (approximately 5000 nt mRNA in length) is expressed in MT-4 cells, we were unable to recover Brd4-CTD from the MT-4 cDNA library [3]. This clearly demonstrates the cDNA bias in the genetic screening. A cDNA library derived from non-T cells does not contain genes specifically expressed in T cells. Thus, we have to explore many more cDNA libraries to completely cover the genetic diversity of human cells. The cDNA libraries isolated from long-term non-progressors of HIV-1-seropositive individuals or from elite controllers might be of particular interest, considering that a dominant innate HIV-1 resistance gene, such as CCR5 delta 32, may partly account for the slow progression of AIDS. Similarly, use of a particular cell line and/or virus strain may bias the results. MT-4 cells are positive for HTLV-1, and are able to support robust HIV-1 replication. MT-4 cells do not express CCR5, and are unable to support R5-tropic HIV-1 strains. What if other T cell lines and R5-tropic viral strains are used? What if we assay the same cDNA library in TZM-bl cells? We plan to address these issues in the future studies.

In conclusion, genome-wide genetic screening is a powerful tool for identifying the regulatory factors of HIV-1 replication and innate HIV-1 resistance factors that limit HIV-1 infection and AIDS progression. The HIV-1-host interactome should also reveal poten-

tial therapeutic molecular targets that may be used to develop novel anti-AIDS drugs to tackle the emerging drug resistant viruses. However, the fact that different experimental systems often yield non-overlapping candidates suggests that we have to explore more experimental systems to fully understand the HIV-1-host interactome. Our T cell-based system provides an alternative tool for identifying novel HIV-1 regulatory factors, and should help us understand the HIV-1-host interaction in more detail.

## Acknowledgements

This work was supported by the Japan Health Science Foundation, the Japanese Ministry of Health, Labor and Welfare, and the Japanese Ministry of Education, Culture, Sports, Science and Technology.

## Conflict of interest statement

The authors state that they have no conflict of interest.

## References

[1] Kawano Y, Yoshida T, Hieda K, Aoki J, Miyoshi H, Koyanagi Y. A lentiviral cDNA library employing lambda recombination used to clone an inhibitor of human immunodeficiency virus type 1-induced cell death. J Virol 2004;78(20):11352–9.
[2] Valente ST, Goff SP. Inhibition of HIV-1 gene expression by a fragment of hnRNP U. Mol Cell 2006;23(4):597–605.
[3] Urano E, Kariya Y, Futahashi Y, Ichikawa R, Hamatake M, Fukazawa H, et al. Identification of the P-TEFb complex-interacting domain of Brd4 as an inhibitor of HIV-1 replication by functional cDNA library screening in MT-4 cells. FEBS Lett 2008;582(29):4053–8.
[4] Yoshida T, Kawano Y, Sato K, Ando Y, Aoki J, Miura Y, et al. A CD63 mutant inhibits T-cell tropic human immunodeficiency virus type 1 entry by disrupting CXCR4 trafficking to the plasma membrane. Traffic 2008;9(4):540–58.
[5] Zhou H, Xu M, Huang Q, Gates AT, Zhang XD, Castle JC, et al. Genome-scale RNAi screen for host factors required for HIV replication. Cell Host Microbe 2008;4(5):495–504.
[6] Brass AL, Dykxhoorn DM, Benita Y, Yan N, Engelman A, Xavier RJ, et al. Identification of host proteins required for HIV infection through a functional genomic screen. Science 2008;319(5865):921–6.
[7] Konig R, Zhou Y, Elleder D, Diamond TL, Bonamy GM, Irelan JT, et al. Global analysis of host-pathogen interactions that regulate early-stage HIV-1 replication. Cell 2008;135(1):49–60.
[8] Valente ST, Gilmartin GM, Mott C, Falkard B, Goff SP. Inhibition of HIV-1 replication by eIF3f. Proc Natl Acad Sci USA 2009;106(11):4071–8.
[9] Aiken C. Pseudotyping human immunodeficiency virus type 1 (HIV-1) by the glycoprotein of vesicular stomatitis virus targets HIV-1 entry to an endocytic pathway and suppresses both the requirement for Nef and the sensitivity to cyclosporin A. J Virol 1997;71(8):5871–7.
[10] Akari H, Uchiyama T, Fukumori T, Iida S, Koyama AH, Adachi A. Pseudotyping human immunodeficiency virus type 1 by vesicular stomatitis virus G protein does not reduce the cell-dependent requirement of vif for optimal infectivity: functional difference between Vif and Nef. J Gen Virol 1999;80(Pt 11):2945–9.
[11] Chazal N, Singer G, Aiken C, Hammarskjold ML, Rekosh D. Human immunodeficiency virus type 1 particles pseudotyped with envelope proteins that fuse at low pH no longer require Nef for optimal infectivity. J Virol 2001;75(8):4014–8.
[12] Komano J, Miyauchi K, Matsuda Z, Yamamoto N. Inhibiting the Arp2/3 complex limits infection of both intracellular mature vaccinia virus and primate lentiviruses. Mol Biol Cell 2004;15(12):5197–207.
[13] Goff SP. Knockdown screens to knockout HIV-1. Cell 2008;135(3):417–20.
[14] Urano E, Aoki T, Futahashi Y, Murakami T, Morikawa Y, Yamamoto N, et al. Substitution of the myristoylation signal of human immunodeficiency virus type 1 Pr55Gag with the phospholipase C-delta1 pleckstrin homology domain results in infectious pseudovirion production. J Gen Virol 2008;89(Pt 12):3144–9.
[15] Futahashi Y, Komano J, Urano E, Aoki T, Hamatake M, Miyauchi K, et al. Separate elements are required for ligand-dependent and–independent internalization of metastatic potentiator CXCR4. Cancer Sci 2007;98(3):373–9.
[16] Zufferey R, Dull T, Mandel RJ, Bukovsky A, Quiroz D, Naldini L, et al. Self-inactivating lentivirus vector for safe and efficient in vivo gene delivery. J Virol 1998;72(12):9873–80.
[17] Shimizu S, Urano E, Futahashi Y, Miyauchi K, Isogai M, Matsuda Z, et al. Inhibiting lentiviral replication by HEXIM1, a cellular negative regulator of the CDK9/cyclin T complex. AIDS 2007;21(5):575–82.
[18] Chinen K, Takahashi E, Nakamura Y. Isolation and mapping of a human gene (SEC14L), partially homologous to yeast SEC14, that contains a variable number of tandem repeats (VNTR) site in its 3' untranslated region. Cytogenet Cell Genet 1996;73(3):218–23.
[19] Howe AG, McMaster CR. Regulation of phosphatidylcholine homeostasis by Sec14. Can J Physiol Pharmacol 2006;84(1):29–38.
[20] Saito K, Tautz L, Mustelin T. The lipid-binding SEC14 domain. Biochim Biophys Acta 2007;1771(6):719–26.
[21] Mousley CJ, Tyeryar KR, Vincent-Pope P, Bankaitis VA. The Sec14-superfamily and the regulatory interface between phospholipid metabolism and membrane trafficking. Biochim Biophys Acta 2007;1771(6):727–36.
[22] Anantharaman V, Aravind L. The GOLD domain, a novel protein module involved in Golgi function and secretion. Genome Biol 2002;3(5), research0023.0021-0023.0027.
[23] Ribeiro FM, Ferreira LT, Marion S, Fontes S, Gomez M, Ferguson SS, et al. SEC14-like protein 1 interacts with cholinergic transporters. Neurochem Int 2007;50(2):356–64.

Journal of Controlled Release 142 (2010) 431–437

Contents lists available at ScienceDirect

Journal of Controlled Release

journal homepage: www.elsevier.com/locate/jconrel



# Prevention of hepatic ischemia–reperfusion injury by pre-administration of catalase-expressing adenovirus vectors

Masahiro Ushitora [a,b], Fuminori Sakurai [a,*], Tomoko Yamaguchi [a,c], Shin-ichiro Nakamura [d], Masuo Kondoh [b], Kiyohito Yagi [b], Kenji Kawabata [a], Hiroyuki Mizuguchi [a,c,*]

[a] Laboratory of Gene Transfer and Regulation, National Institute of Biomedical Innovation, Osaka, Japan
[b] Laboratory of Bio-Functional Molecular Chemistry, Graduate School of Pharmaceutical Sciences, Osaka University, Osaka, Japan
[c] Department of Biochemistry and Molecular Biology, Graduate School of Pharmaceutical Sciences, Osaka University, Osaka, Japan
[d] Research Center of Animal Life Science, Shiga University of Medical Science, Otsu-City, Shiga, Japan

ARTICLE INFO

*Article history:*
Received 17 August 2009
Accepted 25 November 2009
Available online 29 November 2009

*Keywords:*
Adenovirus vector
Reactive oxygen
Ischemia/reperfusion
Liver
Catalase
Hepatectomy

ABSTRACT

Liver ischemia/reperfusion (I/R) injury, which is mainly caused by the generation of reactive oxygen species (ROS) during the reperfusion, remains an important clinical problem associated with liver transplantation and major liver surgery. Therefore, ROS should be detoxified to prevent hepatic I/R-induced injury. Delivery of antioxidant genes into liver is considered to be promising for prevention of hepatic I/R injury; however, therapeutic effects of antioxidant gene transfer to the liver have not been fully examined. The aim of this study was to examine whether adenovirus (Ad) vector-mediated catalase gene transfer in the liver is an effective approach for scavenging ROS and preventing hepatic I/R injury. Intravenous administration of Ad vectors expressing catalase, which is an antioxidant enzyme scavenging $H_2O_2$, resulted in a significant increase in catalase activity in the liver. Pre-injection of catalase-expressing Ad vectors dramatically prevented I/R-induced elevation in serum alanine aminotransferase (ALT) and aspartate aminotransferase (AST) levels, and hepatic necrosis. The livers were also protected in another liver injury model, $CCl_4$-induced liver injury, by catalase-expressing Ad vectors. Furthermore, the survival rates of mice subjected to both partial hepatectomy and I/R treatment were improved by pre-injection of catalase-expressing Ad vectors. On the other hand, control Ad vectors expressing β-galactosidase did not show any significant preventive effects in the liver on the models of I/R-induced or $CCl_4$-induced hepatic injury described above. These results indicate that hepatic delivery of the catalase gene by Ad vectors is a promising approach for the prevention of oxidative stress-induced liver injury.



## 1. Introduction

Hepatic ischemia/reperfusion (I/R) injury occurs in a variety of clinical settings, such as in liver transplantation, hepatic failure after shock, and liver surgery, and results in severe damages that substantially contribute to the morbidity and mortality of such cases [1–3]. Hepatic I/R injury is caused by reactive oxygen species (ROS), including superoxide anion, hydrogen oxide, and hydroxyl radical, which are generated by reperfusion of the ischemic tissue. ROS induce lipid peroxidation and damages to proteins and nucleic acids, leading to parenchymal cell dysfunction and necrosis, increased vascular permeability, and inflammatory cell infiltration [4]. Therefore, ROS should be detoxified to prevent hepatic I/R injury.

In previous animal studies, antioxidative enzyme catalase and superoxide dismutase (SOD) were systemically administered to neutralize ROS and prevent I/R-induced hepatic injury. Although catalase and SOD are endogenously expressed in the cells, the expression levels of these enzymes are insufficient to prevent I/R injury. Administration of antioxidant enzymes exhibited therapeutic effects on ROS-induced diseases, including I/R-induced hepatic injury, in several studies [5–8]; however, these enzymes are known to be rapidly eliminated from the circulation following systemic administration, which limits their therapeutic potential, [9,10] although chemical modification of antioxidant enzymes has been carried out to enhance their plasma half-lives and tissue accessibility [5,6,9]. In addition, systemically administered antioxidant enzymes might be degraded in the endosomes/lysosomes because they are internalized into the cells via the endocytosis pathway.

The delivery of therapeutic genes encoding antioxidant enzymes into the liver is considered to be a promising strategy to overcome these problems. Previous studies have demonstrated that ROS-mediated injury was efficiently prevented by over-expression of antioxidant

* Corresponding authors. Sakurai is to be contacted at Laboratory of Gene Transfer and Regulation, National Institute of Biomedical Innovation, 5-6-7 Saito Asagi, Ibaraki, Osaka, 567-0085, Japan. Tel.: +81 72 641 9815; fax: +81 72 641 9816. Mizuguchi, Department of Biochemistry and Molecular Biology, Graduate School of Pharmaceutical Sciences, Osaka University, 1-6 Yamadaoka, Suita, Osaka, 565-0871, Japan. Tel./fax: +81 6 6879 8185.
*E-mail addresses:* sakurai@nibio.go.jp (F. Sakurai), mizuguch@phs.osaka-u.ac.jp (H. Mizuguchi).

0168-3659/$ – see front matter. 
doi:10.1016/j.jconrel.2009.11.024

enzymes in various tissues, including the artery, pancreatic islets, and brain [11–13]. A variety of types of gene delivery vehicles have been employed for delivery of antioxidative genes so far, and replication-incompetent adenovirus (Ad) vectors have several advantages over other vehicles to deliver antioxidant genes to the liver. First, Ad vectors have high tropism to livers. A more than $10^3$-fold higher transgene expression is found in the liver, compared with other organs, following systemic administration [14–16]. Second, non-dividing cells are efficiently transduced with Ad vectors. Hepatocytes do not actively divide under normal conditions. Non-viral gene delivery vehicles have been used for prevention of hepatic I/R injury in previous studies [17,18]; however, non-viral gene delivery vehicles mediate inefficient transfection in non-dividing cells. Third, the Ad vector genome is not integrated into the host genome, indicating that transduction with Ad vectors is unlikely to induce insertional mutagenesis in hepatocytes. Fourth, Ad vector-mediated gene expression in liver persists for 1–2 weeks, [19,20] in contrast, rapid reduction in plasmid DNA-mediated transgene expression in organs is found after injection of non-viral gene delivery vehicles [21,22]. In spite of these advantages of Ad vectors, the ability of Ad vectors expressing antioxidant enzymes to prevent hepatic I/R injury has not been fully examined probably because Ad vectors are generally considered more toxic than non-viral gene delivery vehicles; however, our group demonstrated that intravenous administration of Ad vectors induces less amounts of inflammatory cytokines than cationic lipid/plasmid DNA complexes [23]. In addition, fiber-modified Ad vectors carrying a stretch of lysine residues in the C-terminus of a fiber knob have been demonstrated to poorly activate innate immune responses after systemic injection, compared with conventional Ad vectors [24]. These results suggest that Ad vectors, including fiber-modified Ad vectors, would be suitable for prevention of I/R injury by delivering antioxidant genes to livers.

Among antioxidant enzymes, SOD is often used for detoxifying ROS in previous studies [8,17,25,26]. SOD catabolizes superoxide anion to $H_2O_2$; however, $H_2O_2$ is converted to hydroxyl radicals, which are extremely reactive and more toxic than other ROS. $H_2O_2$ should be removed to effectively reduce I/R injury. Another antioxidant enzyme, catalase, prevents the generation of hydroxyl radicals by catabolizing $H_2O_2$ to $H_2O$ and $O_2$, suggesting that catalase is promising for prevention of I/R injury. However, there are few studies reporting therapeutic effects of catalase gene delivery on I/R injury [17,27].

In the present study, catalase-expressing Ad vectors were intravenously pre-administered to prevent I/R-induced hepatic injury. Pre-injection of catalase-expressing Ad vectors successfully prevented not only I/R-induced hepatic injury but also $CCl_4$-induced liver damages. Furthermore, mice receiving pre-injection of catalase-expressing Ad vectors showed improved survival rates after partial hepatectomy followed by hepatic I/R.

## 2. Materials and methods

### 2.1. Cells

A549 (a human lung adenocarcinoma epithelial cell line), HepG2 (a human hepatocellular liver carcinoma cell line), and 293 (a human embryonic kidney cell line) cells were cultured in Dulbecco's modified Eagle's medium (DMEM) supplemented with 10% fetal bovine serum under 5% $CO_2$ at 37 °C.

### 2.2. Ad vectors

Ad vectors were constructed by means of an improved *in vitro* ligation method [28–30]. Briefly, the LacZ gene, which is derived from pCMVβ (Marker Gene, Inc., Eugene, OR) and the catalase gene, which is derived from pZEOSV2-CAT (a kind gift from Dr. J. Andres Melendez, Albany Medical College, Albany, NY) [31,32] were inserted into pHMCA5, [33] creating pHMCA5-LacZ and pHMCA5-CAT, respectively. pHMCA5-LacZ and pHMCA5-CAT were then digested with I-CeuI and PI-SceI, and ligated with I-CeuI/PI-SecI-digested pAdHM4 [28], resulting in pAdHM4-LacZ and pAdHM4-CAT, respectively. To generate the viruses, PacI-digested Ad vector plasmids were transfected into 293 cells plated in a 60-mm dish with SuperFect (Qiagen, Inc., Valencia, CA) according to the manufacturer's instructions. The viruses were prepared by the standard method, then purified with $CsCl_2$ gradient centrifugation, dialyzed with a solution containing 10 mM Tris (pH7.5), 1 mM $MgCl_2$, and 10% glycerol, and stored in aliquots at −80 °C. The determinations of infectious titers and virus particle (VP) titers were accomplished using 293 cells and an Adeno-X rapid titer kit (Clontech, Mountain View, CA) and the method of Maizel et al. [34], respectively. Catalase-, or β-galactosidase-expressing fiber-modified Ad vectors carrying a stretch of lysine residues (K7 (KKKKKKK) peptide) in the C-terminus of a fiber knob, AdK7-CAT and AdK7-LacZ, respectively, were similarly prepared using pAdHM41K7 [35]. The ratios of the biological-to-particle titer were 1:20, 1:31, 1:45, and 1:39 for Ad-LacZ, AdK7-LacZ, Ad-CAT, and AdK7-CAT, respectively.

### 2.3. Western blot analysis for catalase expression

A549 cells were transduced with Ad vectors at 3000 VP/cell for 2 h. Forty-eight hours later, cells were harvested and lysed with lysis buffer (20 mM Tris–HCl (pH 8.0), 137 mM NaCl, 1% Triton X-100, 10% glycerol) containing protease inhibitor cocktail (Sigma Chemical., St. Louis, MO). Equal quantities of protein (5 μg), as determined by a protein assay (Bio-Rad, Hercules, CA), were subjected to sodium dodecyl sulfate/12.5% polyacrylamide gel electrophoresis (SDS-PAGE) and transferred onto a polyvinylidene fluoride membrane (Millipore, Bedford, MA). After blocking nonspecific binding, the membrane was incubated with anti-catalase antibody (diluted 1/8000; Calbiochem, San Diego, CA) at room temperature for 3 h, followed by reaction with horse radish peroxidase (HRP)-conjugated anti-rabbit IgG (diluted 1/3000; Cell Signaling Technology, Beverly, MA) at room temperature for 1 h. The band was visualized by ECL Plus Western blotting detection reagents (Amersham Bioscience, Piscataway, NJ), and the signals were read using an LAS-3000 imaging system (Fujifilm, Tokyo, Japan). For detection of the internal control, a polyclonal anti-glyceraldehyde-3-phosphate dehydrogenase antibody (diluted 1/5000; Trevigen, Gaithersburg, MD) and an HRP-conjugated anti-rabbit IgG were used.

### 2.4. In vitro protective effect of catalase-expressing Ad vectors on ROS-induced cell damage

HepG2 cells (5000 cells/well) were seeded onto a 96-well plate. On the following day, the cells were transduced with Ad-LacZ, AdK7-LacZ, Ad-CAT, or AdK7-CAT at 300 or 3000 VP/cell for 2 h. After a 48-h incubation, the medium was exchanged for normal medium containing 30 mM menadione (Sigma Chemical), which is a ROS inducer. On the following day, the cell viability was determined by Alamar blue staining (BioSource, San Diego, CA).

### 2.5. Catalase activities in the liver after intravenous administration of Ad vectors

Ad vectors (Ad-LacZ, AdK7-LacZ, Ad-CAT, and AdK7-CAT) were intravenously administered into C57BL/6 mice (7–8-week-old females; Nippon SLC, Shizuoka, Japan) at a dose of $1 \times 10^{10}$ VP/mice. Forty-eight hours later, the livers were isolated and homogenized with 50 mM potassium phosphate buffer containing 1 mM EDTA. The supernatants were recovered after centrifugation of the homogenates, and catalase activity in the supernatants was measured using a CalBiochem Catalase Assay Kit (Calbiochem).

### 2.6. Hepatic ischemia/reperfusion experiment

Mice were intravenously administered PBS (control) or Ad vectors via the tail vein at a dose of $10^{10}$ VP/mice. A partial hepatic ischemia/reperfusion experiment was performed as previously described [36,37]. Briefly, 2 days post-administration of Ad vectors, mice were anesthetized with a peritoneal injection of pentobarbital sodium (50 mg/kg). An incision was made in the abdomen, and all structures in the portal triad (hepatic artery, portal vein, bile duct) were occluded with a vascular clamp for 1 h to induce hepatic ischemia. Then, blood was allowed to flow through the liver again by removal of the clamp (reperfusion). After an appropriate period of reperfusion (0, 1, 6, 24 h), blood was collected via retro-orbital bleeding, and serum was obtained by centrifugation. The aspartate aminotransferase (ALT) and alanine aminotransferase (AST) activities in serum, as indicators of liver injury during reperfusion, were assayed using a transaminase-CII test (Wako, Osaka, Japan). In separate experiments, histology in the liver sections was evaluated 24 h after reperfusion. The livers were recovered and fixed by immersion in 10% buffered formalin, embedded in paraffin and processed for histology. Tissue damage was assessed in hematoxylin and eosin-stained sections. A sham surgery was performed under anesthesia but without occluding the vessels.

### 2.7. $CCl_4$-induced liver injury experiment

Ad vectors were intravenously administered into mice as described above. Forty-eight hours after Ad vector injection, $CCl_4$ dissolved in olive oil was intraperitoneally administrated to the mice at a dose of 1 ml/kg body weight to induce acute liver failure. Twenty-four hours after $CCl_4$ administration, blood was collected via retro-orbital bleeding, and the levels of ALT and AST in the serum were determined as described above.

### 2.8. Partial hepatectomy

Ad vectors were intravenously administered into mice as described above. Forty-eight hours after Ad vector injection, mice were anesthetized and subjected to two-thirds hepatectomy as described previously [38,39]. Subsequently, liver I/R was conducted by occlusion of the blood vessel to block the blood flow into the remnant liver for 8 min followed by reperfusion as described above. After the surgery, the mice were maintained under conventional conditions to monitor survival rates.

### 2.9. Statistical analysis

Results were expressed as the means ± S.D. Statistically significant differences between groups were determined by the two-way analysis of variance, followed by Student's *t*-test. The levels of statistical significance were set at $p<0.05$ and $p<0.01$.

## 3. Results

### 3.1. Ad vector-mediated catalase expression in vitro

First, to examine *in vitro* catalase expression levels following Ad vector infection, Western blotting analysis was performed. We observed an apparent increase in the catalase expression after transduction with Ad-CAT or AdK7-CAT in A549 cells (Fig. 1). In addition, AdK7-CAT mediated higher catalase expression than Ad-CAT, probably due to the higher transduction activity of AdK7 vectors than conventional Ad vectors [35]. The control Ad vectors, Ad-LacZ and AdK7-LacZ, did not increase catalase expression, indicating that transduction with Ad vectors alone does not induce any change in the antioxidant systems.

Next, to examine whether Ad vector-mediated over-expression of catalase prevents ROS-induced cellular toxicity, the cells were incubated with 30 mM menadione following transduction with Ad vectors, and the cell viabilities were determined. It is well known that menadione produces superoxide radicals in cells, leading to oxidative stress-induced cell death [40,41]. As shown in Fig. 2, the cell viability was significantly reduced to less than 50% in the presence of 30 mM menadione. In contrast, transduction with catalase-expressing Ad vectors dramatically improved the cell viabilities. Transduction with Ad-CAT and AdK7-CAT at 300 VP/cell resulted in cell viabilities of 70.8% and 79.1% of the cell, respectively. These results indicate that Ad vector-mediated over-expression of catalase is beneficial in preventing oxidative stress-induced cell death by efficiently deleting ROS.

### 3.2. Catalase activity in the liver following catalase-expressing Ad vector injection

Next, to measure catalase activities in the liver following intravenous administration of Ad vectors, the livers were recovered 48 h after Ad vector injection, and catalase activities in the liver were determined. The catalase activities were 2.4-fold and 4.3-fold increased following administration of Ad-CAT and AdK7-CAT, respectively (Fig. 3). By contrast, we found no elevation in the catalase activity by LacZ-expressing Ad vectors. These results indicate that catalase activity in the liver is significantly elevated by intravenous administration of catalase-expressing Ad vectors.

### 3.3. Prevention of hepatic I/R injury by pre-administration of catalase-expressing Ad vectors

To evaluate the ability of catalase-expressing Ad vectors to prevent hepatic I/R injury, serum ALT and AST levels were measured after 1 h of hepatic ischemia followed by reperfusion. Both serum ALT and AST levels were highly elevated at 1 h and 6 h after the reperfusion of hepatic flows in the mice pre-injected with PBS, indicating that hepatic injury was induced by I/R (Fig. 4). At 1 h after reperfusion, the ALT and AST levels increased from 59.3 to 184.0 and from 421.2 to 1174.7 IU/L, respectively. However, pretreatment with Ad-CAT or AdK7-CAT significantly reduced the serum ALT and AST levels at 6 h after reperfusion. The ALT and AST levels in mice pre-injected with AdK7-CAT were 3.9- and 4.4-fold lower than those in mice pre-injected with PBS. Reductions in the ALT and AST levels were also observed at 1 h after reperfusion, although these changes were not statistically significant. The control Ad vectors, Ad-LacZ and AdK7-LacZ, exhibited no suppressive effects on the I/R-induced elevation of serum ALT and AST levels.

Furthermore, to histologically evaluate the preventive effects of catalase-expressing Ad vectors, liver sections were prepared 24 h after reperfusion. An extensive necrotic area was observed in the mice pretreated with PBS or AdK7-LacZ (Fig. 5B, C). In contrast, transduction with Ad-CAT or AdK7-CAT resulted in a dramatic decrease in the necrotic area induced by hepatic I/R (Fig. 5D, E). In particular,

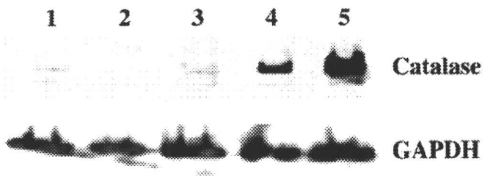


**Fig. 1.** Catalase expression following Ad vector transduction. A549 cells were transduced with Ad-LacZ, Ad-CAT, or AdK7-CAT at 3000 VP/cell for 2 h. Protein samples were collected after a 48-h incubation and analyzed by Western blotting. Lane 1, mock; lane 2, Ad-LacZ; lane 3, AdK7-LacZ; lane 4, Ad-CAT; lane 5, AdK7-CAT. The results are representative of two

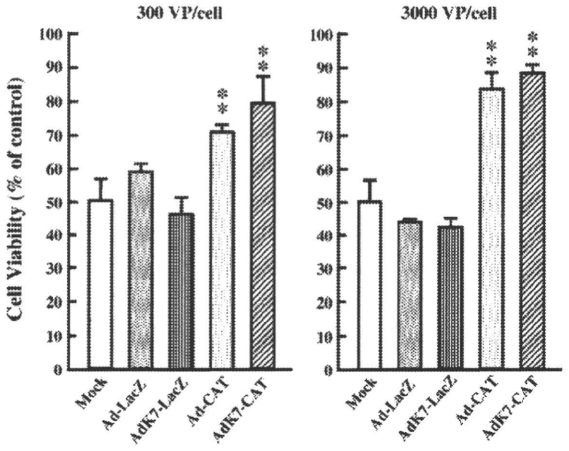


**Fig. 2.** Protective effects of catalase-expressing Ad vectors against menadione-induced cell death. HepG2 cells were transduced with Ad vectors at 300 or 3000 VP/cell for 2 h. After a 48-h incubation, menadione was added to the medium at a final concentration of 30 mM, and the cells were cultured for an additional 24 h. The cellular viabilities were then determined by Alamar blue staining. The cellular viabilities were normalized to the viability of Ad vector-infected HepG2 cells in the absence of menadione. The data are expressed as the means ± S.D. ($n = 4$). **Significantly different from the mock-infected group at $p < 0.01$.

pre-injection of AdK7-CAT almost completely prevented necrosis in the liver, although there were several small necrotic areas in the liver pretreated with Ad-CAT, probably due to the higher transduction efficiency and less liver toxicity profile of AdK7 vectors in the liver compared with conventional Ad vectors [24]. A TUNEL assay indicated that Ad-CAT and AdK7-CAT prevented the DNA fragmentation caused by hepatic I/R in hepatocytes (data not shown). These results indicate that the I/R-induced histological damages were also significantly attenuated by pretreatment with catalase-expressing Ad vectors.

### *3.4. Preventive effect of catalase-expressing Ad vectors on $CCl_4$-induced liver injury*

To explore whether Ad vector-mediated catalase expression prevents other types of oxidative stress-induced liver injury, $CCl_4$ was intraperitoneally injected into mice pretreated with catalase-expressing Ad vectors. $CCl_4$ is well known to produce $CCl_3$ radical, leading to acute liver injury. Serum ALT and AST levels were highly elevated following $CCl_4$ treatment in mice pretreated with PBS or LacZ-expressing Ad vectors (Fig. 6). However, serum ALT and AST levels were markedly reduced by pretreatment with Ad-CAT and AdK7-CAT. AdK7-CAT mediated a 4.9-fold and 3.9-fold reduction in serum ALT and AST levels, respectively, compared with PBS. Ad-CAT and AdK7-CAT also mediated a dramatic improvement of $CCl_4$-induced gross abnormality in the liver (data not shown). These results indicate that catalase-expressing Ad vectors possess preventive effects on oxidative stress-induced injury that are distinct from their effects on I/R injury.

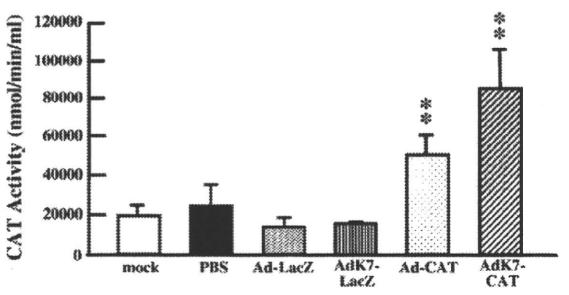


**Fig. 3.** Catalase activity in the liver following intravenous administration of catalase-expressing Ad vectors. Ad vectors were administered to mice at the dose of $1 \times 10^{10}$ VP/mouse. The livers were recovered 48 h after injection, and catalase activities in mouse liver homogenates were determined. The data are expressed as the means ± S.D. ($n = 5$). **Significantly different from the mock-infected group at $p < 0.01$.

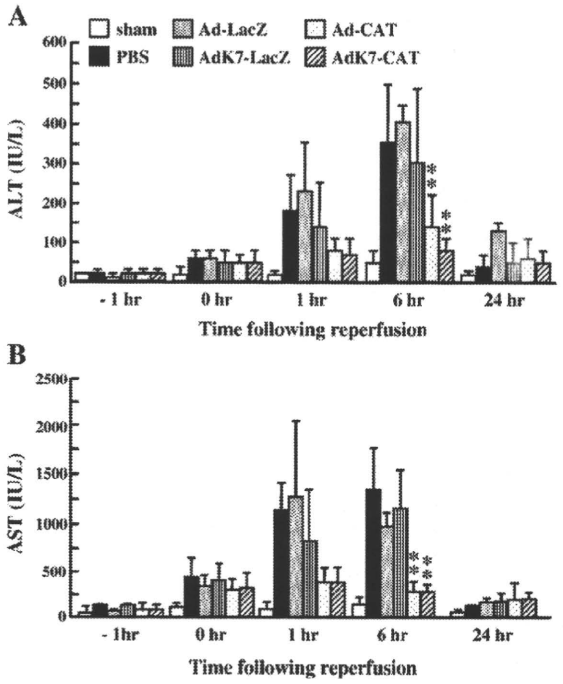


**Fig. 4.** Effects of pre-administration of catalase-expressing Ad vectors on serum ALT (A) and AST (B) levels in mice following hepatic ischemia/reperfusion injury. Ad vectors were intravenously administered to mice at a dose of $1 \times 10^{10}$ VP/mice. Forty-eight hours after Ad vector injection, mice were subjected to a 1 h period of ischemia followed by hepatic reperfusion. Serum samples were taken at 1 h before ischemia, and 0, 1, 6, and 24 h after reperfusion. The data are expressed as the mean ± S.E. ($n = 3$–8). **Significantly different from the PBS-injected group at $p < 0.01$.

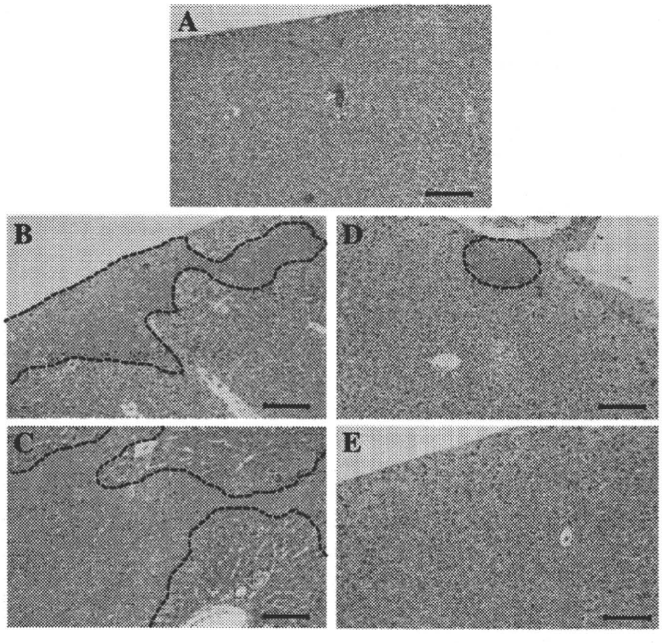


**Fig. 5.** Representative images of liver sections of mice 24 h following hepatic ischemia/reperfusion. A) Sham, B) PBS, C) AdK7-LacZ, D) Ad-CAT, and E) AdK7-CAT. Mice were subjected to hepatic I/R 48 h after Ad vector injection, as described in Fig. 4. Livers were recovered 24 h after I/R treatment, and liver sections stained with hematoxylin and eosin were observed under a microscope. A dashed line indicates the necrotic area. The scale bar represents 100 μm.

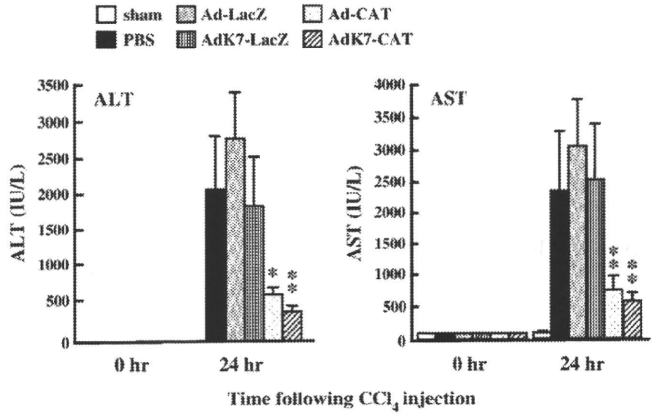


**Fig. 6.** Preventive effect of catalase-expressing Ad vectors on $CCl_4$-induced acute liver failure. $CCl_4$ (1 ml/kg) was intraperitoneally injected to mice 48 h following Ad vector injection. Serum samples were collected 24 h after $CCl_4$ administration. The data are expressed as the means ± S.D. ($n=4$). *Significantly different from the PBS-injected group at $p<0.05$; ** at $p<0.01$.

### 3.5. Improvement of survival rates of mice subjected to partial hepatectomy and hepatic ischemia/reperfusion by catalase-expressing Ad vectors

To examine whether over-expression of catalase improves the remnant liver function in mice subjected to both partial hepatectomy and I/R treatment, partial hepatectomy and subsequent I/R treatment were conducted 48 h after pre-administration of Ad vectors. Partial hepatectomy is often performed under hepatic ischemia, and the remaining liver suffers from I/R injury after partial hepatectomy in clinical settings. Mice pre-administered with AdK7-CAT showed a dramatic improvement in survival rate (Fig. 7). Seventy percent of mice survived for 7 days after these treatments. The body weights of the mice pre-injected with AdK7-CAT were not significantly reduced 7 days after surgery, compared with those before surgery (data not shown), suggesting that the general health of the mice was not substantially compromised after the surgery. On the other hand, the survival of the mice was not prolonged by pre-administration of Ad-LacZ or PBS. These results indicate that catalase-expressing Ad vectors are able to protect the liver from more serious stress induced by partial hepatectomy and I/R, and to improve the remnant liver function.

## 4. Discussion

Hepatotoxins, drugs, and I/R can injure the liver via oxidative stress. With the aim of efficiently preventing oxidative stress-induced hepatic injury, we pre-administered Ad vectors expressing an antioxidative enzyme, catalase, to mice. The results of our study demonstrated that Ad vector-mediated over-expression of catalase in the liver effectively prevents hepatic injury caused by not only I/R but also $CCl_4$. Furthermore, the survival rates of mice subjected to both partial hepatectomy and I/R treatment were prolonged by over-expression of catalase.

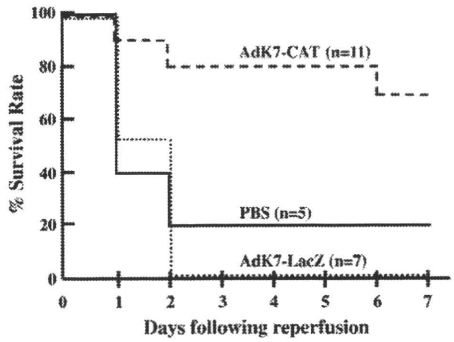


**Fig. 7.** Survival rates of mice subjected to partial hepatectomy and hepatic I/R following Ad vector administration. Solid line: PBS ($n=5$); dotted line: AdK7-LacZ ($n=7$); dashed line: AdK7-CAT ($n=11$). Ad vectors were intravenously administered to mice as described in Fig. 4. Forty-eight hours after Ad vector administration, mice were subjected to two-thirds partial hepatectomy, followed by an 8 min-period of ischemia

Superoxide anion is the primary oxidant species generated during hepatic I/R by a xanthine oxidase system and/or decoupling of the electron transport system in mitochondria. Superoxide anion is readily converted to $H_2O_2$ by SOD or a spontaneous reaction. $H_2O_2$ itself is a weak oxidizing agent; however, hydroxyl radical is produced by $H_2O_2$ in the presence of transition-metal ion. Hydroxyl radical has the most oxidative ability and the strongest toxicity among the various ROS. Reduction/elimination of hydroxyl radical is considered to be the most effective strategy for prevention of hepatic I/R injury. Therefore, catalase, which prevents generation of hydroxyl radical by converting $H_2O_2$ to $H_2O$ and $O_2$, was selected as the antioxidant enzyme in the present study. Catalase derivatives also exhibited higher preventive effects on the elevation of serum ALT and AST levels induced by hepatic I/R, compared with SOD derivatives [5,6]. In addition, over-expression of catalase in the liver might increase endogenous expression of SOD, which is another advantage of catalase gene transfer. He et al. demonstrated that delivery of catalase gene alone to the liver induced SOD activity in the liver [17].

Partial hepatectomy is often performed under hepatic ischemia. Previous studies have shown that oxidative stress induced by hepatic I/R affects hepatocyte cell death and inhibits liver regeneration [42,43]. Beyer et al. reported that ROS are directly responsible for the impairment of insulin/insulin-like growth factor 1 signaling, which is crucial for liver regeneration [44]. Furthermore, hepatocytes without catalase activity have been found in regenerating livers after partial hepatectomy [45], suggesting that hepatocytes in the regenerating livers might be susceptible for ROS-mediated injury. The present study demonstrated that over-expression of catalase in the liver dramatically improved the survival rates of mice subjected to partial hepatectomy and I/R, suggesting that the remnant livers would be protected from ROS-mediated injury by over-expression of catalase. Furthermore, over-expression of catalase might play an important role in maintenance of the regenerative capacity of hepatocytes. Recently, removal of ROS by antioxidant enzymes was demonstrated to be crucial for maintenance of the self-renewal capacity of progenitor/stem cells in an *in vitro* culture system [46,47]. In this study, the liver/body weight ratio of mice pre-injected with AdK7-CAT 1 week after partial hepatectomy and I/R was 4.7 ± 0.55%, which is not significantly different from that of naïve mice (data not shown).

Oxidative stress is also generated in the liver through metabolism of a variety of drugs, chemicals, and toxins, such as thioacetamide, lipopolysaccharide, and $CCl_4$. In particular, $CCl_4$ is often used as a representative hepatotoxin causing oxidative stress in animal experiments. $CCl_4$ is metabolized by cytochrome P450 in the endoplasmic reticulum of hepatocytes, leading to generation of $CCl_3$ radical, which induces hepatic damages, although the mechanism of $CCl_4$-mediated liver damage has not yet been fully revealed. The present study showed that Ad vector-mediated over-expression of catalase in the liver also attenuated $CCl_4$-induced liver injury (Fig. 6). Over-expression of SOD has also been shown to inhibit $CCl_4$-induced hepatic damages [48]. Hepatic delivery of genes encoding ROS-deleting enzymes is effective in case of hepatic injury induced by oxidative stress-generating hepatotoxins and chemical compounds.

Ad vectors offer various advantages for gene delivery to the liver; however, systemic administration of Ad vectors often induces inflammatory cytokine production and hepatic damage [24,49–51]. However, we found no apparent Ad vector-induced damages in the liver in this study (data not shown). Moreover, mice pre-administered Ad-LacZ or AdK7-LacZ did not exhibit higher levels of serum ALT and AST after I/R than those pre-administered PBS (Fig. 4). This was likely

due to the relatively low dose of Ad vectors ($1 \times 10^{10}$ VP/mouse) used in this study. Higher doses of Ad vectors have often been administered in the studies reporting Ad vector-mediated *in vivo* toxicities [49,51]. We confirmed that more than 90% of hepatocytes were efficiently transduced even at a dose of $1 \times 10^{10}$ VP/mouse in this study (data not shown). In general, Ad vectors have been considered more toxic than non-viral vectors containing plasmid DNA; however, our group recently revealed that Ad vectors induced smaller amounts of inflammatory cytokines, which are partly involved in Ad vector-induced hepatic toxicity, following intravenous administration into mice, compared with plasmid DNA/cationic liposome complexes, which were used as a representative of non-viral gene delivery vehicle [23]. In both that previous study and our present work, Ad vectors successfully deliver antioxidant genes to the liver with no apparent toxicity, although we should pay attention to the vector doses.

In addition to conventional Ad vectors, fiber-modified AdK7 vectors, which display a poly-lysine motif on the c-terminal of the fiber knob, [24,35,52] were used in this study. AdK7 vectors mediate not only significantly higher transgene expression in the liver but also lower *in vivo* damages than conventional Ad vectors [24]. However, the serum ALT and AST levels of the mice receiving Ad-CAT and AdK7-CAT were not significantly different from those of the controls in this study (Fig. 4), although histological analysis of the liver sections revealed that AdK7-CAT conferred superior protection against I/R injury (Fig. 5), probably because sufficient levels of catalase would be expressed by Ad-CAT at this dose to prevent hepatic I/R-induced increases in serum ALT and AST in this setting. AdK7-CAT might show higher protective effects than conventional Ad vectors under more severe conditions.

In conclusion, the present study demonstrated that Ad vector-mediated catalase expression in the liver significantly improved I/R-induced hepatic injury. These findings suggests that Ad vectors expressing antioxidant enzymes would contribute to the development of strategies aimed at inhibiting hepatic I/R injury. Antioxidant enzyme-expressing Ad vectors are also applicable for the prevention of I/R-induced injury in other organs and oxidative stress-induced damages caused by ROS-generating chemicals. Moreover, their combined use with other antioxidant genes or anti-apoptosis genes could further attenuate oxidative stress-induced injury.

## Acknowledgement

We thank Dr. Yuriko Higuchi (Graduate School of Pharmaceutical Sciences, Kyoto University, Kyoto, Japan) for her help in the liver ischemia/reperfusion experiments. We also thank Dr. Kazuo Ohashi (Institute of Advanced Biomedical Engineering and Sciences, Tokyo Women's Medical University, Tokyo, Japan) for his help in the partial hepatectomy experiment. This work was supported by grants from the Ministry of Health, Labour, and Welfare of Japan.

## References

[1] R.G. Thurman, et al., Hepatic reperfusion injury following orthotopic liver transplantation in the rat, Transplantation 46 (1988) 502–506.
[2] J.M. McCord, Oxygen-derived free radicals in postischemic tissue injury, N. Engl. J. Med. 312 (1985) 159–163.
[3] M.J. Arthur, et al., Oxygen-derived free radicals promote hepatic injury in the rat, Gastroenterology 89 (1985) 1114–1122.
[4] D.N. Granger, R.J. Korthuis, Physiologic mechanisms of postischemic tissue injury, Annu. Rev. Physiol. 57 (1995) 311–332.
[5] Y. Yabe, et al., Prevention of neutrophil-mediated hepatic ischemia/reperfusion injury by superoxide dismutase and catalase derivatives, J. Pharmacol. Exp. Ther. 298 (2001) 894–899.
[6] Y. Yabe, et al., Targeted delivery and improved therapeutic potential of catalase by chemical modification: combination with superoxide dismutase derivatives, J. Pharmacol. Exp. Ther. 289 (1999) 1176–1184.
[7] S.L. Atalla, L.H. Toledo-Pereyra, G.H. MacKenzie, J.P. Cederna, Influence of oxygen-derived free radical scavengers on ischemic livers, Transplantation 40 (1985) 584–590.
[8] T. Fujita, et al., Therapeutic effects of superoxide dismutase derivatives modified with mono- or polysaccharides on hepatic injury induced by ischemia/reperfusion, Biochem. Biophys. Res. Commun. 189 (1992) 191–196.
[9] P.S. Pyatak, A. Abuchowski, F.F. Davis, Preparation of a polyethylene glycol: superoxide dismutase adduct, and an examination of its blood circulation life and anti-inflammatory activity, Res. Commun. Chem. Pathol. Pharmacol. 29 (1980) 113–127.
[10] J.F. Turrens, J.D. Crapo, B.A. Freeman, Protection against oxygen toxicity by intravenous injection of liposome-entrapped catalase and superoxide dismutase, J. Clin. Invest. 73 (1984) 87–95.
[11] L. Agrawal, et al., Antioxidant enzyme gene delivery to protect from HIV-1 gp120-induced neuronal apoptosis, Gene Ther. 13 (2006) 1645–1656.
[12] P.Y. Benhamou, et al., Adenovirus-mediated catalase gene transfer reduces oxidant stress in human, porcine and rat pancreatic islets, Diabetologia 41 (1998) 1093–1100.
[13] E. Durand, et al., Adenovirus-mediated gene transfer of superoxide dismutase and catalase decreases restenosis after balloon angioplasty, J. Vasc. Res. 42 (2005) 255–265.
[14] F. Sakurai, H. Mizuguchi, T. Yamaguchi, T. Hayakawa, Characterization of in vitro and in vivo gene transfer properties of adenovirus serotype 35 vector, Mol. Ther. 8 (2003) 813–821.
[15] H. Mizuguchi, et al., CAR- or alphav integrin-binding ablated adenovirus vectors, but not fiber-modified vectors containing RGD peptide, do not change the systemic gene transfer properties in mice, Gene Ther. 9 (2002) 769–776.
[16] R. Alemany, D.T. Curiel, CAR-binding ablation does not change biodistribution and toxicity of adenoviral vectors, Gene Ther. 8 (2001) 1347–1353.
[17] S.Q. He, et al., Delivery of antioxidative enzyme genes protects against ischemia/reperfusion-induced liver injury in mice, Liver Transpl. 12 (2006) 1869–1879.
[18] H. Yin, et al., Pretreatment with soluble ST2 reduces warm hepatic ischemia/reperfusion injury, Biochem. Biophys. Res. Commun. 351 (2006) 940–946.
[19] R.S. Sung, L. Qin, J.S. Bromberg, TNFalpha and IFNgamma induced by innate anti-adenoviral immune responses inhibit adenovirus-mediated transgene expression, Mol. Ther. 3 (2001) 757–767.
[20] N. Morral, et al., Immune responses to reporter proteins and high viral dose limit duration of expression with adenoviral vectors: comparison of E2a wild type and E2a deleted vectors, Hum. Gene Ther. 8 (1997) 1275–1286.
[21] S. Li, L. Huang, In vivo gene transfer via intravenous administration of cationic lipid–protamine–DNA (LPD) complexes, Gene Ther. 4 (1997) 891–900.
[22] S. Li, et al., Effect of immune response on gene transfer to the lung via systemic administration of cationic lipidic vectors, Am. J. Physiol. 276 (1999) L796–L804.
[23] H. Sakurai, et al., Comparison of gene expression efficiency and innate immune response induced by Ad vector and lipoplex, J. Control. Release 117 (2007) 430–437.
[24] N. Koizumi, et al., Fiber-modified adenovirus vectors decrease liver toxicity through reduced IL-6 production, J. Immunol. 178 (2007) 1767–1773.
[25] M.D. Wheeler, et al., Comparison of the effect of adenoviral delivery of three superoxide dismutase genes against hepatic ischemia–reperfusion injury, Hum. Gene Ther. 12 (2001) 2167–2177.
[26] S. Kondo, et al., Mannosylated superoxide dismutase inhibits hepatic reperfusion injury in rats, J. Surg. Res. 60 (1996) 36–40.
[27] B. Chen, et al., Delivery of antioxidant enzyme genes protects against ischemia/reperfusion-induced injury to retinal microvasculature, Invest. Ophthalmol. Vis. Sci. 50 (2009) 5587–5595.
[28] H. Mizuguchi, M.A. Kay, Efficient construction of a recombinant adenovirus vector by an improved in vitro ligation method, Hum. Gene Ther. 9 (1998) 2577–2583.
[29] H. Mizuguchi, M.A. Kay, A simple method for constructing E1- and E1/E4-deleted recombinant adenoviral vectors, Hum. Gene Ther. 10 (1999) 2013–2017.
[30] H. Mizuguchi, et al., A simplified system for constructing recombinant adenoviral vectors containing heterologous peptides in the HI loop of their fiber knob, Gene Ther. 8 (2001) 730–735.
[31] M. Mari, J. Bai, A.I. Cederbaum, Adenovirus-mediated overexpression of catalase in the cytosolic or mitochondrial compartment protects against toxicity caused by glutathione depletion in HepG2 cells expressing CYP2E1, J. Pharmacol. Exp. Ther. 301 (2002) 111–118.
[32] J. Bai, A.I. Cederbaum, Adenovirus-mediated overexpression of catalase in the cytosolic or mitochondrial compartment protects against cytochrome P450 2E1-dependent toxicity in HepG2 cells, J. Biol. Chem. 276 (2001) 4315–4321.
[33] F. Sakurai, et al., Optimization of adenovirus serotype 35 vectors for efficient transduction in human hematopoietic progenitors: comparison of promoter activities, Gene Ther. 12 (2005) 1424–1433.
[34] J.V. Maizel Jr., D.O. White, M.D. Scharff, The polypeptides of adenovirus. I. Evidence for multiple protein components in the virion and a comparison of types 2, 7A, and 12, Virology 36 (1968) 115–125.
[35] N. Koizumi, et al., Generation of fiber-modified adenovirus vectors containing heterologous peptides in both the HI loop and C terminus of the fiber knob, J. Gene Med. 5 (2003) 267–276.
[36] A. Tsung, et al., The nuclear factor HMGB1 mediates hepatic injury after murine liver ischemia–reperfusion, J. Exp. Med. 201 (2005) 1135–1143.
[37] M.R. Duranski, et al., Cytoprotective effects of nitrite during in vivo ischemia–reperfusion of the heart and liver, J. Clin. Invest. 115 (2005) 1232–1240.
[38] K. Ohashi, F. Park, M.A. Kay, Role of hepatocyte direct hyperplasia in lentivirus-mediated liver transduction in vivo, Hum. Gene Ther. 13 (2002) 653–663.
[39] K. Ohashi, et al., Liver tissue engineering at extrahepatic sites in mice as a potential new therapy for genetic liver diseases, Hepatology 41 (2005) 132–140.
[40] T.J. Monks, et al., Quinone chemistry and toxicity, Toxicol. Appl. Pharmacol. 112 (1992) 2–16.
[41] H. Thor, et al., The metabolism of menadione (2-methyl-1, 4-naphthoquinone) by isolated hepatocytes. A study of the implications of oxidative stress in intact cells, J. Biol. Chem. 257 (1982) 12419–12425.
[42] N. Fausto, Liver regeneration, J. Hepatol. 32 (2000) 19–31.

[43] H. Kamata, et al., Reactive oxygen species promote TNFalpha-induced death and sustained JNK activation by inhibiting MAP kinase phosphatases, Cell 120 (2005) 649–661.
[44] T.A. Beyer, et al., Impaired liver regeneration in Nrf2 knockout mice: role of ROS-mediated insulin/IGF-1 resistance, Embo J. 27 (2008) 212–223.
[45] I. Oikawa, P.M. Novikoff, Catalase-negative peroxisomes: transient appearance in rat hepatocytes during liver regeneration after partial hepatectomy, Am. J. Pathol. 146 (1995) 673–687.
[46] R.C. Meagher, A.J. Salvado, D.G. Wright, An analysis of the multilineage production of human hematopoietic progenitors in long-term bone marrow culture: evidence that reactive oxygen intermediates derived from mature phagocytic cells have a role in limiting progenitor cell self-renewal, Blood 72 (1988) 273–281.
[47] R. Gupta, S. Karpatkin, R.S. Basch, Hematopoiesis and stem cell renewal in long-term bone marrow cultures containing catalase, Blood 107 (2006) 1837–1846.
[48] S.K. Venugopal, et al., Lentivirus-mediated superoxide dismutase1 gene delivery protects against oxidative stress-induced liver injury in mice, Liver Int. 27 (2007) 1311–1322.
[49] M. Christ, et al., Modulation of the inflammatory properties and hepatotoxicity of recombinant adenovirus vectors by the viral E4 gene products, Hum. Gene Ther. 11 (2000) 415–427.
[50] A. Lieber, et al., Inhibition of NF-kappaB activation in combination with bcl-2 expression allows for persistence of first-generation adenovirus vectors in the mouse liver, J. Virol. 72 (1998) 9267–9277.
[51] R.S. Everett, et al., Liver toxicities typically induced by first-generation adenoviral vectors can be reduced by use of E1, E2b-deleted adenoviral vectors, Hum. Gene Ther. 14 (2003) 1715–1726.
[52] T.J. Wickham, et al., increased in vitro and in vivo gene transfer by adenovirus vectors containing chimeric fiber proteins, j. virol. 71 (1997) 8221–8229.

doi: 10.1111/j.1365-3083.2010.02416.x

# Intradermal Delivery of Recombinant Vaccinia Virus Vector DIs Induces Gut-Mucosal Immunity

N. Yoshino*†, M. Kanekiyo†, Y. Hagiwara‡, T. Okamura†, K. Someya†, K. Matsuo†, Y. Ami§, S. Sato*, N. Yamamoto† & M. Honda†

*Department of Microbiology, School of Medicine, Iwate Medical University, Iwate; †AIDS Research Center, National Institute of Infectious Diseases, Tokyo; ‡Research Center for Biologicals, The Kitasato Institute, Saitama; and §Division of Experimental Animals Research, National Institute of Infectious Diseases, Tokyo, Japan

*Received 15 March 2010; Accepted in revised form 29 April 2010*

*Correspondence to*: N. Yoshino, Department of Microbiology, School of Medicine, Iwate Medical University, 19-1 Uchimaru, Morioka, Iwate 020-8505, Japan. E-mail: nyoshino@iwate-med.ac.jp

## Abstract

Antigen-specific mucosal immunity is generally induced by the stimulation of inductive mucosal sites. In this study, we found that the replication-deficient vaccinia virus vector, DIs, generates antigen-specific mucosal immunity and systemic responses. Following intradermal injection of recombinant DIs expressing simian immunodeficiency virus *gag* (rDIsSIV*gag*), we observed increased levels of SIV p27-specific IgA and IgG antibodies in faecal extracts and plasma samples, and antibody-forming cells in the intestinal mucosa and spleen of C57BL/6 mice. Antibodies against p27 were not detected in nasal washes, saliva, and vaginal washes. The enhanced mucosal and systemic immunity persisted for 1 year of observation. Induction of Gag-specific IFN-$\gamma$ spot-forming $CD8^+$ T cells in the spleen, small intestinal intraepithelial lymphocytes, and submandibular lymph nodes was observed in the intradermally injected mice. Heat-inactivated rDIsSIV*gag* rarely induced antigen-specific humoral and T-helper immunity. Moreover, rDIsSIV*gag* was detected in MHC class II IA antigen-positive ($IA^+$) cells at the injection site. Consequently, intradermal delivery of rDIs effectively induces antigen-specific humoral and cellular immunity in gut-mucosal tissues of mice. Our data suggest that intradermal injection of an rDIs vaccine may be useful against mucosally transmitted pathogens.

## Introduction

As most infectious agents, including human immunodeficiency virus (HIV), are often transmitted via mucosal surfaces, a mucosal-inductive vaccine capable of eliciting protective immunity in mucosal tissues and external secretions would act as the first line of defence at the site of initial invasion. For inducting preventive immunity to HIV, a vaccine must induce anti-HIV neutralizing antibodies (Ab) and/or cytotoxic T lymphocytes against HIV-infected cells in the mucosal and submucosal areas [1]. Parenterally immunized vaccines generally do not enhance the levels of secretory IgA Ab production in external secretions and are less able to induce the mucosal immune responses needed to prevent infection at the site of initial contact between the host and the infectious agent [2–4].

Poxvirus vectors are among the most heavily exploited for vaccine development. Their use is largely attributable to the overwhelming success of the vaccinia virus vaccine in eradicating smallpox. Because of concerns regarding the use of a replicating vector in immunocompromised individuals, non-replicating poxvirus vectors, such as the modified vaccinia virus Ankara (MVA) [5], are an area of interest for extensive development. The replication-deficient vaccinia virus, DIs, is a candidate viral vector; and it is a safe and highly attenuated mutant of the vaccinia virus [6–9]. When recombinant DIs (rDIs) encoding foreign antigens (Ag) was intravenously [9, 10], intramuscularly [11, 12], subcutaneously [13], or intradermally [14] injected, Ag-specific systemic immunity was induced in mice and non-human primates.

Activation of the inductive sites is of paramount importance to induce Ag-specific mucosal immunity. Intradermal and intramuscular injection of a DNA vaccine generates solely systemic but rarely mucosal responses [15, 16]. The potential importance of specific mucosal immunity in the protection against mucosally transmitted pathogens is beginning to emerge from many investigations. We had previously demonstrated that intranasal or intragastrical administration of rDIs encoding full-length simian immunodeficiency virus *gag*

(rDIsSIV*gag*) could induce Gag-specific cytotoxic T lymphocytes and p27-specific Ab in both the systemic sites and the mucosal sites of mice [17].

In recent clinical studies, the smallpox vaccine was administered by skin scarification, subcutaneous, intramuscular, or intradermal vaccination [18–20]. Immunization of the mice with MVA by skin scarification protected the mice against intranasal challenge with pathogenic Western Reserve vaccinia virus in mice, but intramuscular immunization was ineffective [21]. Subcutaneous injection of rDIs was inefficient to induce Ag-specific mucosal IgA Ab responses whereas high IgG Ab responses were induced in the plasma [13]. DIs vaccines are typically parenterally injected; however, mucosal immunity has not been tested in parenterally injected animals. An advantage of intradermal injection is that all the materials for intradermal injection are readily available and accessible to clinicians. Therefore, we studied whether intradermal injection of rDIs induces mucosal immunity. Here, we describe the enhanced induction of humoral and cellular immunity in the mucosal tissues of mice injected intradermally with the DIs vector.

## Materials and methods

*Recombinant vaccinia virus vectors.* The production and preparation of rDIsSIV*gag* and rDIs expressing LacZ (rDIsLacZ) as a control vector have been described in detail previously [9, 11]. To prepare heat-inactivated rDIsSIV*gag*, $10^5$ PFU of rDIsSIV*gag* was incubated at 56 °C for 30 min. The PFU of heat-inactivated rDIsSIV*gag* was confirmed as < 2 by a chicken embryo fibroblast culture [22, 23]. These vectors were stored at −80 °C until used.

*Mice.* Five-week-old C57BL/6N mice were purchased from Charles River Japan, Inc. (Yokohama, Japan). The mice were acclimated to the experimental animal facility for more than 1 week before being used in the experiments. They were maintained in the facility under pathogen-free conditions. All experimental procedures were performed in accordance with the guidelines established by the National Institute of Infectious Diseases, Japan. The study was conducted in a biosafety level 2 facility under the approval of an institutional committee for biosafety and in accordance with the requirements of the World Health Organization. In cases of specification, systemic vaccination against pathogenic viruses or bacteria induced mucosal secretory IgA Ab responses in individuals who had previously been exposed to its pathogen by the mucosal route [24–26]. That, of course, is negated here because we used naive mice in this study, and p27-specific Ab were not detected in the plasma and faecal extracts of the mice before immunization.

*Immunization.* The mice were injected intradermally at the interscapular region thrice at weekly intervals in two contiguous sites with a 25-μl aliquot of PBS containing $10^5$ PFU per 50 μl of rDIsSIV*gag* or rDIsLacZ. The mice were extensively washed with warm water, blot-dried, and then washed and dried again to avoid acquiring small amounts of injected rDIs through their normal grooming activity. To compare with the mucosal immunization, the mice were immunized with $10^5$ PFU of rDIsSIV*gag* by the nasal route thrice at weekly intervals according to previously described methods [17].

*Sample collection and preparation of single-cell suspensions.* After immunization, blood and mucosal secretions (faecal extracts, nasal washes, saliva, and vaginal washes) were collected by using methods described elsewhere [27–30]. Vaginal washes were pooled from four mice for each experiment [30]. The collected samples were stored at −80 °C until used. Single-cell suspensions were obtained from the spleen, mesenteric lymph nodes (MLN), submandibular lymph nodes (SMLN), axillary lymph nodes (ALN), small intestinal lamina propria (i-LP), and small intestinal intraepithelial lymphocytes (IEL) as previously described [29].

*Analysis of IFN-γ production of SIV Gag peptide-specific $CD8^+$ T cells.* To detect Gag-specific cellular immunity, $CD8^+$ T cells in the spleen, IEL, and SMLN of mice were cultured with or without overlapping Gag peptide. The methods of $CD8^+$ T cell enrichment and Gag-specific IFN-γ spot-forming cells (SFC) assessed by enzyme-linked immunosorbent spot (ELISPOT) assay were as described previously [17]. The number of Gag-specific IFN-γ SFC was calculated by subtracting the results of the control culture (i.e. without Gag peptide stimulation) from those of the peptide-stimulated culture, because non-specific activated $CD8^+$ T cells produced IFN-γ.

*Detection of SIV p27-specific Ab production by ELISA and enumeration of p27-specific Ab-forming cells by ELISPOT assay.* Titres of p27-specific Ab in the plasma and mucosal secretions were determined by an endpoint enzyme-linked immunosorbent assay (ELISA). The endpoint titres were expressed as the last dilution that gave an optical density at 450 nm ($OD_{450}$) of ≥ 0.1 OD units above the $OD_{450}$ of the negative controls [17]. SIV p27-specific IgA, IgG, and IgM Ab-forming cells (AFC) in the spleen, i-LP, and MLN of mice were determined by ELISPOT assay. SIV p27-specific AFC were quantitated with the aid of a stereomicroscope [17].

*Cytokine production of SIV Gag peptide-specific $CD4^+$ T cells.* Overlapping Gag peptide-specific helper immunity of $CD4^+$ T cells in the spleen of mice was measured by ELISA. The methods of $CD4^+$ T-cell purification and culture conditions were as described previously [17]. The levels of IFN-γ, IL-4, and IL-10 were measured by ELISA kit (eBioscience, San Diego, CA, USA). The levels of Gag-specific IFN-γ, IL-4, and IL-10 in the culture supernatants were calculated by subtracting the results of the

control cultures from those of the Gag peptide-stimulated cultures.

*Isolation of IA$^+$ cells in the skin.* Twenty-four hours after the intradermal injection of $10^7$ PFU rDIsSIV*gag*, the mice were shaved at the vaccinal locus with a razor. The skin was then removed and cut to approximately $1 \times 1$ cm$^2$ of the vaccinal locus. MHC class II IA antigen-positive (IA$^+$) cells were isolated from the skin by enzymatic dissociation protocols [31]. The epidermal cells were incubated with anti-I-A$^b$ monoclonal Ab (AF6-120.1; Becton Dickinson, San José, CA, USA). IA$^+$ cells were isolated by auto MACS (Miltenyi Biotec GmbH, Bergisch Gladbach, Germany). The purified fractions included > 97% IA$^+$ cells.

*Preparation of DNA samples and amplification of SIV gag* gene by nested PCR. For determining the distribution of rDIsSIV*gag*, a nested PCR was used to amplify a fragment of the *gag* gene segment. DNA samples were prepared from the skin, skin IA$^+$ cells, ALN, SMLN, Peyer's patches (PP) and spleen. The preparation, amplification methods, and primer sequences are described elsewhere [17, 32]. The lowest concentration of plasmid SIV DNA detectable with this PCR method in the first amplification with an outer *gag* primer pair was $10^3$ copies. Upon further amplification with nested/internal *gag* primers, a single copy of plasmid DNA could be routinely detected [32].

*Statistical analysis.* Normally distributed variables were compared by the two-tailed Student's *t*-test, and the results are expressed as the mean ± the standard deviation (SD). Non-normally distributed variables were compared by the two-tailed Mann–Whitney *U* test, and the results are expressed as the median and the interquartile range (IQR). A $P$ value < 0.05 was considered significant.

## Results

### Cellular and humoral immunity by intradermal injection of rDIs

The first step was to assess whether intradermal injection of rDIsSIV*gag* induces Gag-specific IFN-γ-producing CD8$^+$ T cells in mucosal and systemic tissues. Although the BCG vector itself non-specifically enhances the levels of some cytokines [33], the DIs empty vector and rDIs-LacZ scarcely stimulated IFN-γ-production, and the number of IFN-γ SFC per $10^6$ cells was less than 32 in intradermally injected mice [14] and intramuscularly injected non-human primates [12] in our previous studies. Moreover, the calculated number of Gag-specific IFN-γ SFC from naive mice was < 15 per $10^6$ CD8$^+$ T cells. A calculated number of SFC above 15 was considered positive. The number of Gag-specific IFN-γ SFC in the spleen in the intradermal injection group was significantly higher than that of the mice immunized intranasally with the same dose of rDIsSIV*gag*. Conversely, the number of IFN-γ SFC in the IEL of the mice injected intradermally was significantly lower than that of the intranasally immunized mice. There was no significant difference in the SMLN between the intradermally injected group and the intranasally immunized group (Fig. 1). Gag-specific IFN-γ-producing CD8$^+$ T cells were apparent in both mucosal and systemic tissues in the intradermally injected mice.

Ag-specific Ab, especially secretory IgA Ab in mucosal secretions, have been shown to be of central importance for host defence [1, 34]. We assessed the Ab response to p27 in the plasma and faecal extracts of immunized mice at 1 week after the last immunization. Intradermal injection of rDIsSIV*gag* induced p27-specific IgG Ab in the plasma, and p27-specific IgA Ab in the faecal extracts in six of the eight (75%) mice at 1 week after the last intradermal injection. Remarkably, the titres of p27-specific IgA Ab in the faecal extracts of mice immunized intradermally or intranasally with rDIsSIV*gag* were roughly equivalent (Fig. 2). However, p27-specific IgA Ab were not detected in the nasal washes, saliva, and vaginal washes of intradermally injected mice (data not shown). The p27-specific IgG and IgA Ab titres in the plasma and faecal extracts from the mice intradermally injected with rDIsLacZ (negative controls) were less than the detection limit on endpoint ELISA among (data not shown).

Intragastric immunization with rDIsSIV*gag* has been reported to induce p27-specific IgA Ab in the faecal

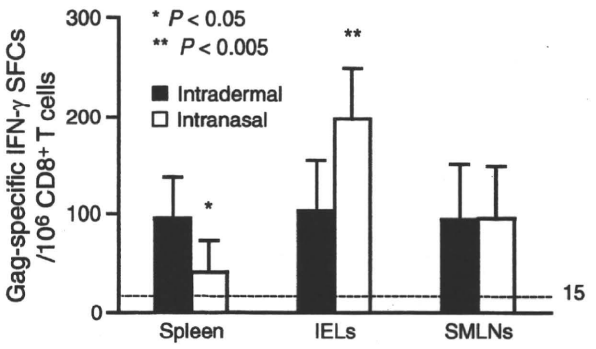


**Figure 1** Intradermal injection of rDIsSIV*gag* induced SIV Gag-specific IFN-γ-secreted CD8$^+$ T cells in both mucosal tissues and systemic tissue. CD8$^+$ T cells were isolated one week after the last injection from the spleen, IEL, and SMLN of the mice injected intradermally (closed column) or intranasally (open column) with $10^5$ PFU of rDIsSIV*gag*. IFN-γ production was assessed by ELISPOT assay. The number of Gag-specific IFN-γ SFC was calculated by subtracting the results of the control culture from those of the peptide-stimulated culture. The data are shown as the mean number of SFC per $10^6$ CD8$^+$ T cells + SD for eight mice in each group and are representative of two separate experiments. Each group was compared by two-tailed Student's *t*-test. Significant differences between the intranasal group and the intradermal group are indicated with an asterisk (*$P$ < 0.05, **$P$ < 0.005).

 

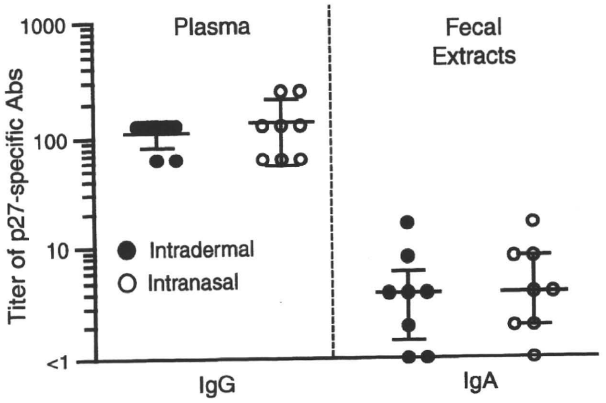


Figure 2 Intradermal injection of rDIsSIV*gag* induced SIV p27-specific Ab in the plasma. The mice were killed one week after the last immunization. The titres of p27-specific IgG Ab in the plasma and IgA Ab in the faecal extracts of the mice injected intradermally or intranasally with $10^5$ PFU of rDIsSIV*gag* were determined by ELISA. Each dot represents an individual mouse. The horizontal and vertical bars indicate the mean ± SD for eight mice in each experimental group and are representative of two separate experiments. The titre of the IgG Ab in the plasma of each group was compared by two-tailed Student's *t*-test, and the titre of the IgA Ab in the faecal extracts of each group was compared by the two-tailed Mann–Whitney *U* test.

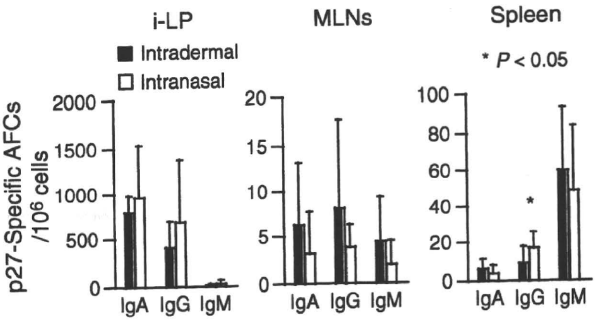


Figure 3 Intradermal injection of rDIsSIV*gag* induced SIV p27-specific AFC in the mucosal and systemic tissues. The mice were killed one week after the last immunization. The levels of p27-specific IgA, IgG, and IgM AFC in the i-LP, MLN, and spleen of the mice injected intradermally (closed column) or intranasally (open column) with $10^5$ PFU of rDIsSIV*gag* were determined by ELISPOT assay. The data are shown as the mean number of AFC per $10^6$ cells + SD for eight mice and representative of two separate experiments. The number of AFCs in the tissues of each group was compared by two-tailed Student's *t*-test.

extracts of mice at 1 week after the last immunization [17]. IgA Ab against p27 were detected in four of the eight (50%) mice that were intragastrically administered $10^5$ PFU of rDIsSIV*gag*, and the range of the IgA Ab titre was < 2–32 [17]. The statistical significance of the differences among the three groups was assessed using Kruskal–Wallis test ($P$ = 0.6818). We found that intradermal injection of rDIsSIV*gag* induced p27-specific IgA Ab in the faecal extracts at similar titres as observed after intranasal and intragastric immunization among mice receiving the same dose.

We also assessed the number of p27-specific AFC induced in the i-LP, MLN, and spleen after intradermal injection of rDIsSIV*gag*. We found clear evidence of p27-specific IgA AFC in the i-LP of the mice injected intradermally with rDIsSIV*gag*. The AFC were detected in the i-LP and MLN of mice intradermally injected with rDIsSIV*gag*, with similar levels of the IgA AFC observed for intranasal group receiving the same dose. Only the number of p27-specific IgG AFC in the spleen significantly differed among the intradermal and intranasal groups (Fig. 3). No p27-specific AFC were detected in the tested tissues of the mice intradermally injected with rDIsLacZ (data not shown).

### Assessment of long-lasting p27-specific Ab production by intradermal rDIs injection

As long-lived memory B and T cells are responsible for the long-lasting immunity elicited by smallpox vaccination in humans [35, 36], we investigated the duration of p27-specific long-lasting humoral immune responses in the systemic and mucosal sites of the mice intradermally injected with rDIsSIV*gag*. 1 week after the last injection, titres of p27-specific IgG Ab were detected in the plasma and peaked at 17–25 weeks. Thereafter, the Ab titres were maintained in the plasma until 49 weeks of testing (~ 1 year) without further boosting (Fig. 4A). Interestingly, p27-specific IgM Ab were observed in the plasma of these mice throughout the 1-year period (Fig. 4A). The levels of p27-specific IgA Ab did not correlate with those of IgG and IgM Ab; increases in p27-specific IgA Ab titres were observed until 11 weeks after the last injection. After peaking, IgA Ab were barely detected in the plasma for 1 year, and the mean titre of IgA Ab in the intradermally injected mice declined to a value between 22 and 56 (Fig. 4A).

After that p27-specific IgA Ab were detected in the faecal extracts from six of eight mice at 1 week; these Ab were detected in the faecal extracts of all the mice at 11 and 25 weeks. Moreover, the Ab in the faecal extracts were detected after approximately 1 year in four of eight (50%) mice (Fig. 4B). Although p27-specific IgG Ab in the faecal extracts were also detected at 1 week after the last injection, they were not observed at 25 and 49 weeks (Fig. 4B).

### Intradermal injection of heat-inactivated rDIs

Mice were intradermally injected with live or heat-inactivated rDIsSIV*gag* and killed at 1 week after the last injection. The mean number of p27-specific IgA AFC in the i-LP of the mice intradermally injected with live and heat-inactivated rDIsSIV*gag* was 788.4 and 12.5 AFC per $10^6$ cells, respectively. SIV p27-specific AFC in all the assessed tissues were scarcely induced in the mice injected

 

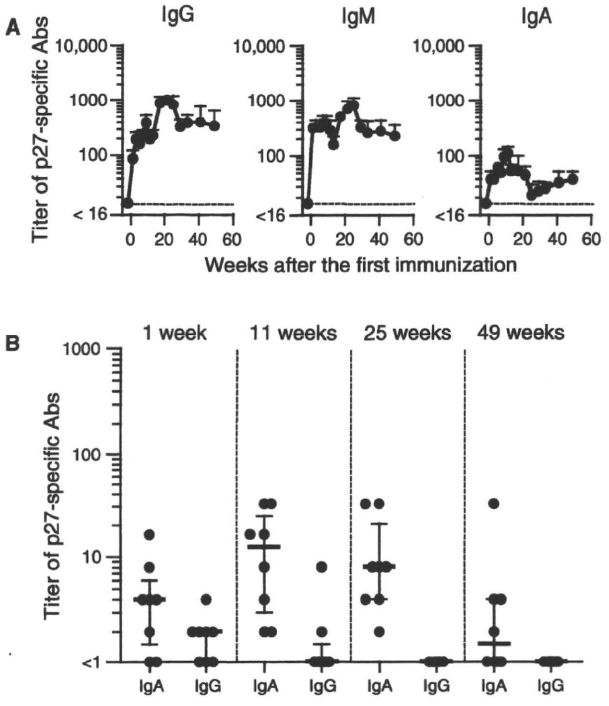


**Figure 4** Intradermal injection of rDIsSIV*gag* induced long-lasting humoral immune responses. The mice were intradermally injected with $10^5$ PFU of rDIsSIV*gag*. Plasma p27-specific IgG, IgM, and IgA Ab (A) and IgA and IgG Ab in faecal extracts (B) were determined by an end-point ELISA. Plasma Ab are shown as the mean titres + SD for eight mice. Faecal pellets were collected at 1, 11, 25, and 49 weeks after the last injection. Each dot in (B) represents an individual mouse. The horizontal and vertical bars indicate the median and IQR. The data are representative of two separate experiments.

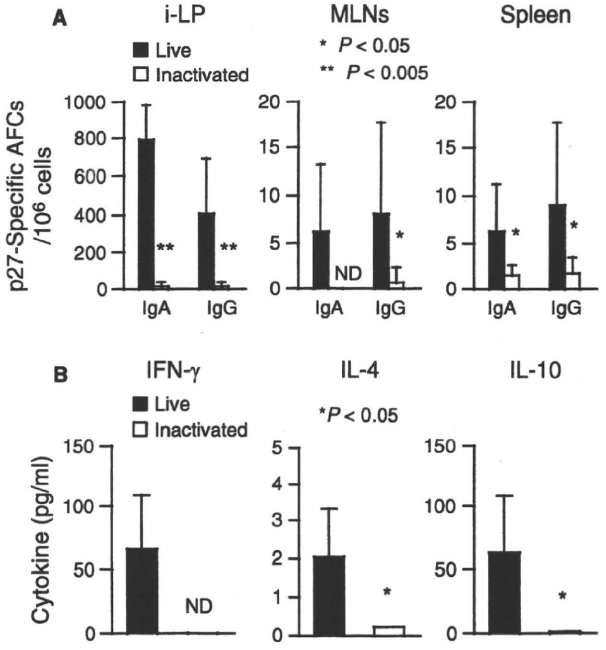


**Figure 5** Intradermal injection of heat-inactivated rDIsSIV*gag* did not induce SIV Gag-specific immunity. (A) The mice were intradermally injected with $10^5$ PFU of rDIsSIV*gag* (closed column) or heat-inactivated rDIsSIV*gag* (open column) and were killed 1 week after the last injection. The levels of p27-specific IgA and IgG AFC in the i-LP, MLN, and spleen were determined by ELISPOT assay. (B) $CD4^+$ T cells were isolated from the spleen 1 week after the last injection. Culture supernatants were harvested and then analysed by ELISA for the production of IFN-γ, IL-4, and IL-10. The data are shown as the mean number of AFC per $10^6$ cells or the mean concentration of cytokines + SD for eight mice in each experimental group and are representative of two separate experiments. Each group was compared by two-tailed Student's *t*-test. Significant differences between the live rDIs group and the heat-inactivated rDIs group are indicated with an asterisk (*$P$ < 0.05, **$P$ < 0.005). ND: not detected.

with inactivated rDIsSIV*gag* (Fig. 5A). Furthermore, we assessed the Gag-specific T helper (Th1)-type and Th2-type responses. Intradermal injection of live rDIsSIV*gag* resulted in effective helper T-cell responses. In contrast, Gag-specific Th2-type responses (IL-4 and IL-10) in the mice injected with inactivated rDIsSIV*gag* were significantly lower than those in the mice injected with live rDIsSIV*gag*. Further, Th1-type responses (IFN-γ) were not detected in the mice injected with inactivated rDIsSIV*gag* (Fig. 5B).

### Distribution of rDIs following intradermal injection

The skin is the ideal site for vaccination because of the presence of Ag-presenting cells such as the Langerhans cells (LC) and dermal dendritic cells (DC) expressing IA MHC class II antigen [37]. When the mice were killed at 1 day after intradermal injection, the *gag* gene was detected in the skin around the injection site. The gene was also detected in the $IA^+$ cells isolated from the skin injected with rDIsSIV*gag*. In the lymphoid tissues, the *gag* gene was detected in the ALN and SMLN of six of the eight (75%) mice. However, the gene was not detected in the spleen and PP of mice by nested PCR at this time point (Fig. 6).

## Discussion

We have demonstrated here that intradermal injection of rDIs could induce Ag-specific immune responses detectable in both the mucosal tissues and systemic tissue of mice. The longevity and stability of immune memory is one of the key factors in vaccine development. In this study, p27-specific IgA Ab in the faecal extracts and plasma IgG Ab immune responses persisted for 1 year of observation. Moreover, IgM Ab against p27 in the plasma were detected throughout the period of Ab monitoring. However, the mechanism governing prolonged p27-specific Ab induction including the IgM subclass has yet to be elucidated. We theorize that sufficient quantities of Gag were continuously produced in the mice to reactivate IgM Ab production in the

 

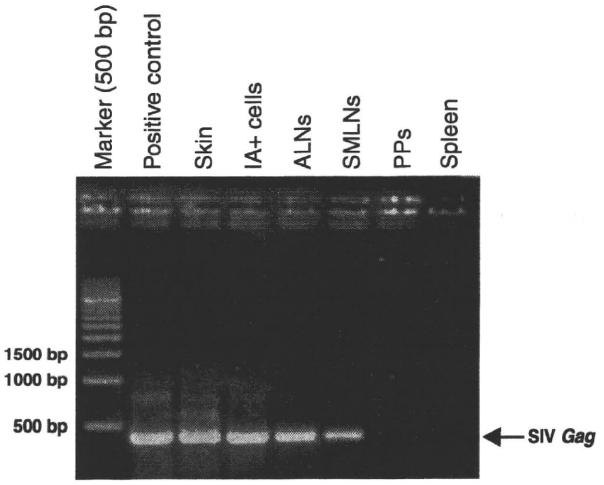


Figure 6 Distribution of rDIsSIV*gag* in the intradermally injected mice. The mice were intradermally injected with $10^7$ PFU of rDIsSIV*gag* and killed 1 day after injection. The *gag* gene was assessed in the skin, $IA^+$ cells, ALN, SMLN, PP, and spleen by nested PCR. The gene was detected in the skin and $IA^+$ cells of all eight mice, in the ALN and SMLN of six mice, but never in the PP and spleen. Amplification with the first-round primers resulted in a band at 613 bp and amplification with the nested primers resulted in a band at 405 bp.

absence of viral replication and reinfection, although we did not assess long-lasting rDIs vector persistence in the mucosal tissues.

Intradermal injection of rMVA induced Ag-specific IgA Ab in faecal extracts and lung washes [38]. It is important to consider that plasma-derived transport of dimeric or polymeric IgA Ab from the systemic circulation into the gut via hepatobiliary transport can influence the titre of IgA Ab in faecal extracts, because of a large portion of murine gut IgA Ab is derived from blood rather than mucosal production [39–41]. Our previous study had showed that intragastric immunization with rDIsSIV*gag* induced p27-specific IgA AFC in i-LP (mean number of IgA AFC, 1994 ± 317) [17]. The number of p27-specific IgA AFC in the i-LP of mice intradermally immunized rDIsSIV*gag* was significantly lower than that in the intragastric group ($P$ = 0.0041). However, the titres of p27-specific IgA Ab in the faecal extracts of mice immunized intradermally or intragastrically with rDIs were roughly equivalent ($P$ = 0.645). Oral immunization induces substantial Ab responses in the small intestine [42, 43]. Intranasal immunization evokes Ab responses in the upper airway mucosa and regional secretions, but not in the gut [44, 45]. Although we could not determine which mucosal tissue(s) produce large amounts of dimeric or polymeric IgA Ab against specific Ag by intradermal injection, our findings validate the notion that intradermal injection of rDIs induces a good level of Ag-specific IgA Ab in the intestinal mucosa.

In this study, the mechanism(s) underlying the induction of immune responses against foreign Ag at mucosal sites by the intradermal injection of the rDIs vector was unclear. The *gag* gene was detected in $IA^+$ cells isolated from skin injected with rDIsSIV*gag*; heat-inactivated rDIsSIV*gag* rarely induces Ag-specific immune responses. These findings may be key in elucidating the above-mentioned mechanism of immune response induction. Further, intradermal passive transfer of rDIsSIV*gag*-infected $IA^+$ cells induced intestinal mucosal immunity against p27 (unpublished data). These findings suggest that $IA^+$ LC and/or dermal DC may be one of the responsible cells for the induction of gut-mucosal immunity, and immune induction may require an activated molecular viral life cycle of rDIs.

Intradermal and intranasal immunization with rDIsSIV*gag* induced Gag-specific IFN-$\gamma$ SFC in SMLN. SMLN contribute to the mucosal immune responses [46, 47] and are one of the secondary lymphoid tissues for mucosal immunity on intranasal immunization [48]. The *gag* gene was detected in the SMLN; however, it remains to be confirmed whether LC, DC, and/or other skin immunity-associated cells [49–52] transfer the rDIsSIV*gag* into draining SMLN. In a study of transcutaneous immunization, langerin$^+$ DC in MLN were found to play a key role in the mutual relationship between the skin immune system and the gut immune system [53]. The *gag* gene was also detected in the ALN. The ALN might be one of the regional LNs in mice injected intradermally in the interscapular region, and systemic immune responses might be activated in the ALN. To investigate the association between intradermal injection and gut mucosa, activated lymphocytes and Ag-presenting cells in the draining LNs of mice should be assessed in future studies.

In conclusion, this study has shown that intradermal delivery of a recombinant vaccinia virus vector, DIs, induces gut-mucosal immunity in mice. However, the observed titres of IgA Ab in the faecal extracts and IgG Ab in the plasma of the mice injected with rDIs alone were not very high. Further, there is no conclusive evidence whether intradermal injection of rDIs provides adequate specific immunity against mucosally transmitted pathogens at mucosal sites. Within the limitations of our study, however, we have shed light on the intradermal route of rDIs injection to induce mucosal immunity and provided an important step towards the development of an effective intradermal rDIs vaccine against mucosally transmitted agents.

## Acknowledgment

This work was supported by the Human Science Foundation of Japan, and the Japanese Ministry of Health, Labor, and Welfare. A part of this work was supported by a grant from the Keiryokai Research Foundation (No. 94). The authors declare no conflict of interest.

## References


1 Letvin NL. Progress and obstacles in the development of an AIDS vaccine. *Nat Rev Immunol* 2006;12:930–9.

2 Ogra PL, Karzon DT, Righthand F *et al.* Immunoglobulin response in serum and secretions after immunization with live and inactivated poliovaccine and natural infection. *N Engl J Med* 1968;279:893–900.

3 Ogra PL, Chiba Y, Beutner KR, Morag A. Vaccination by non-parenteral routes: characteristics of immune response. *Dev Biol Stand* 1976;33:19–26.

4 Kiyono H, Czerkinsky C. Consideration of mucosally induced tolerance in vaccine development. In: Kiyono H, Ogra PL, McGhee JR, eds. *Mucosal Vaccine*. San Diego: Academic Press, 1996:89–101. ISBN: 0-12-410580-7

5 Moss B. Genetically engineered poxviruses for recombinant gene expression, vaccination, and safety. *Proc Natl Acad Sci USA* 1996;93:11341–8.

6 Tagaya I, Kitamura T, Sano Y. A new mutant of dermovaccinia virus. *Nature* 1961;192:381–2.

7 Kitamura T, Kitamura Y. Interference with the growth of vaccinia virus by an attenuated mutant virus. *Jpn J Med Sci Biol* 1963;16:343–57.

8 Kitamura T, Kitamura Y, Tagaya I. Immunogenicity of an attenuated strain of vaccinia virus on rabbits and monkeys. *Nature* 1967;215:1187–8.

9 Ishii K, Ueda Y, Matsuo K *et al.* Structural analysis of vaccinia virus DIs strain: application as a new replication-deficient viral vector. *Virology* 2002;302:433–44.

10 Ami Y, Izumi Y, Matsuo K *et al.* Priming-boosting vaccination with recombinant *Mycobacterium bovis* Bacillus Calmette-Guérin and a nonreplicating vaccinia virus recombinant leads to long-lasting and effective immunity. *J Virol* 2005;79:12871–9.

11 Someya K, Xin KQ, Matsuo K *et al.* A consecutive priming-boosting vaccination of mice with simian immunodeficiency virus (SIV) *gag/pol* DNA and recombinant vaccinia virus strain DIs elicits effective anti-SIV immunity. *J Virol* 2004;78:9842–53.

12 Someya K, Ami Y, Nakasone T *et al.* Induction of positive cellular and humoral immune responses by a prime-boost vaccine encoded with simian immunodeficiency virus *gag/pol*. *J Immunol* 2006;176:1784–95.

13 Ishii K, Hasegawa H, Nagata N *et al.* Induction of protective immunity against severe acute respiratory syndrome coronavirus (SARS-CoV) infection using highly attenuated recombinant vaccinia virus DIs. *Virology* 2006;351:368–80.

14 Okamura T, Someya K, Matsuo K, Hasegawa A, Yamamoto N, Honda M. Recombinant vaccinia DIs expressing simian immunodeficiency virus gag and pol in mammalian cells induces efficient cellular immunity as a safe immunodeficiency virus vaccine candidate. *Microbiol Immunol* 2006;50:989–1000.

15 McCluskie MJ, Davis HL. Novel strategies using DNA for the induction of mucosal immunity. *Crit Rev Immunol* 1999;19:303–29.

16 Stevceva L, Abimiku AG, Franchini G. Targeting the mucosa: genetically engineered vaccines and mucosal immune responses. *Genes Immun* 2000;1:308–15.

17 Yoshino N, Kanekiyo M, Hagiwara Y *et al.* Mucosal administration of completely non-replicative vaccinia virus recombinant Dairen I strain elicits effective mucosal and systemic immunity. *Scand J Immunol* 2008;68:476–83.

18 Frey SE, Newman FK, Yan L, Lottenbach KR, Belshe RB. Response to smallpox vaccine in persons immunized in the distant past. *JAMA* 2003;289:3295–9.

19 Greenberg RN, Kennedy JS, Clanton DJ *et al.* Safety and immunogenicity of new cell-cultured smallpox vaccine compared with calf-lymph derived vaccine: a blind, single-centre, randomised controlled trial. *Lancet* 2005;365:398–409.

20 Kennedy JS, Greenberg RN. IMVAMUNE: modified vaccinia Ankara strain as an attenuated smallpox vaccine. *Expert Rev Vaccines* 2009;8:13–24.

21 Liu L, Zhong Q, Tian T, Dubin K, Athale SK, Kupper TS. Epidermal injury and infection during poxvirus immunization is crucial for the generation of highly protective T cell-mediated immunity. *Nat Med* 2010;16:224–7.

22 Tagaya I, Amano H, Yuasa T. Improved plaque assay of a mutant of vaccinia virus, strain DIs, in chick embryo cell cultures. *Jpn J Med Sci Biol* 1974;27:245–7.

23 Morita M, Aoyama Y, Arita M *et al.* Comparative studies of several vaccinia virus strains by intrathalamic inoculation into cynomolgus monkeys. *Arch Virol* 1977;53:197–208.

24 Svennerholm AM, Holmgren J, Hanson LA, Lindblad BS, Quereshi F, Rahimtoola RJ. Boosting of secretory IgA antibody responses in man by parenteral cholera vaccination. *Scand J Immunol* 1977;6:1345–9.

25 Svennerholm AM, Hanson LA, Holmgren J, Lindblad BS, Nilsson B, Quereshi F. Different secretory immunoglobulin A antibody responses to cholera vaccination in Swedish and Pakistani women. *Infect Immun* 1980;30:427–30.

26 Svennerholm AM, Hanson LA, Holmgren J *et al.* Antibody responses to live and killed poliovirus vaccines in the milk of Pakistani and Swedish women. *J Infect Dis* 1981;143:707–11.

27 Wu HY, Russell MW. Induction of mucosal immunity by intranasal application of a streptococcal surface protein antigen with the cholera toxin B subunit. *Infect Immun* 1993;61:314–22.

28 Tamura S, Miyata K, Matsuo K *et al.* Acceleration of influenza virus clearance by Th1 cells in the nasal site of mice immunized intranasally with adjuvant-combined recombinant nucleoprotein. *J Immunol* 1996;156:3892–900.

29 Moldoveanu Z, Fujihashi K. Collection and processing of external secretions and tissues of mouse origin. In: Mestecky J, Lamm ME, McGhee JR, Bienenstock J, Mayer L, Strober W, eds. *Mucosal Immunology*, 3rd edn. San Diego: Academic Press, 2005:1841–52.

30 Yoshino N, Fujihashi K, Hagiwara Y *et al.* Co-administration of cholera toxin and apple polyphenol extract as a novel and safe mucosal adjuvant strategy. *Vaccine* 2009;27:4808–17.

31 Schuler G, Steinman RM. Murine epidermal Langerhans cells mature into potent immunostimulatory dendritic cells *in vitro*. *J Exp Med* 1985;161:526–46.

32 Unger RE, Marthas ML, Lackner AA *et al.* Detection of simian immunodeficiency virus DNA in macrophages from infected rhesus macaques. *J Med Primatol* 1992;21:74–81.

33 Pelizon AC, Martins DR, Zorzella-Pezavento SFG *et al.* Neonatal BCG immunization followed by DNAhsp65 boosters: highly immunogenic but not protective against tuberculosis – a paradoxical effect of the vector? *Scand J Immunol* 2010;71:63–9.

34 Brandtzaeg P. Mucosal immunity: induction, dissemination, and effector functions. *Scand J Immunol* 2009;70:505–15.

35 Crotty S, Felgner P, Davies H, Glidewell J, Villarreal L, Ahmed R. Cutting edge: long-term B cell memory in humans after smallpox vaccination. *J Immunol* 2003;171:4969–73.

36 Combadiere B, Boissonnas A, Carcelain G *et al.* Distinct time effects of vaccination on long-term proliferative and IFN-γ-producing T cell memory to smallpox in humans. *J Exp Med* 2004;199:1585–93.

37 Romani N, Ratzinger G, Pfaller K *et al.* Migration of dendritic cells into lymphatics-the Langerhans cell example: routes, regulation, and relevance. *Int Rev Cytol* 2001;207:237–70.

38 Wyatt LS, Belyakov IM, Earl PL, Berzofsky JA, Moss B. Enhanced cell surface expression, immunogenicity and genetic stability result-


 

ing from a spontaneous truncation of HIV Env expressed by a recombinant MVA. *Virology* 2008;372:260–72.
39 Vaerman JP, Langendries A, Giffroy D, Brandtzaeg P, Kobayashi K. Lack of SC/pIgR-mediated epithelial transport of a human polymeric IgA devoid of J chain: *in vitro* and *in vivo* studies. *Immunology* 1998;95:90–6.
40 Meckelein B, Externest D, Schmidt MA, Frey A. Contribution of serum immunoglobulin transudate to the antibody immune status of murine intestinal secretions: influence of different sampling procedures. *Clin Diagn Lab Immunol* 2003;10:831–4.
41 Brandtzaeg P. Induction of secretory immunity and memory at mucosal surfaces. *Vaccine* 2007;25:5467–84.
42 Quiding M, Nordström I, Kilander A *et al.* Intestinal immune responses in humans. Oral cholera vaccination induces strong intestinal antibody responses and interferon-gamma production and evokes local immunological memory. *J Clin Invest* 1991;88:143–8.
43 Kozlowski PA, Cu-Uvin S, Neutra MR *et al.* Comparison of the oral, rectal, and vaginal immunization routes for induction of antibodies in rectal and genital tract secretions of women. *Infect Immun* 1997;65:1387–94.
44 Johansson EL, Bergquist C, Edebo A *et al.* Comparison of different routes of vaccination for eliciting antibody responses in the human stomach. *Vaccine* 2004;22:984–90.
45 Johansson EL, Wassén L, Holmgren J *et al.* Nasal and vaginal vaccinations have differential effects on antibody responses in vaginal and cervical secretions in humans. *Infect Immun* 2001;69:7481–6.
46 Mestecky J. The common mucosal immune system and current strategies for induction of immune responses in external secretions. *J Clin Immunol* 1987;7:265–76.
47 Kiyono H, Fukuyama S. NALT- versus Peyer's-patch-mediated mucosal immunity. *Nat Rev Immunol* 2004;4:699–710.
48 Fujihashi K, Staats HF, Kozaki S, Pascual DW. Mucosal vaccine development for botulinum intoxication. *Expert Rev Vaccines* 2007;6:35–45.
49 Streilein JW. Skin-associated lymphoid tissue. *Immunol Ser* 1989;46:73–96.
50 Sontheimer RD. Perivascular dendritic macrophages as immunobiological constituents of the human dermal microvascular unit. *J Invest Dermatol* 1989;93:96S–101S.
51 Bos JD, Kapsenberg ML. The skin immune system: progress in cutaneous biology. *Immunol Today* 1993;14:75–8.
52 Nestle FO, Nickoloff BJ. A fresh morphological and functional look at dermal dendritic cells. *J Cutan Pathol* 1995;22:385–93.
53 Chang SY, Cha HR, Igarashi O *et al.* Cutting edge: Langerin$^+$ dendritic cells in the mesenteric lymph node set the stage for skin and gut immune system cross-talk. *J Immunol* 2008;180:4361–5.